ACS APPLIED NANO MATERIALS

www.acsanm.org

Review

Review of MXene-Based Electrospun Nanocomposites for Flexible and Wearable Sensors

Ashfaqul Hoque Khadem, Habibur Rahman Anik,* Md Golam Mortuza Limon, Mahbubay Rabbani, Abu Sayed Rafi, Israt Khandaker Mim, Md Habibur Rahman, Faisal Bin Alam, Md Khayrul Islam, Syeda Shirajum Munira, Md Touhidul Islam, Mohsin Uddin, and Hrishita Mony

Cite This: *ACS Appl. Nano Mater.* 2025, 8, 16231−16259

Read Online

ACCESS | Metrics & More | Article Recommendations | Supporting Information

ABSTRACT: The necessity for achieving high-performance and precise detection of internal and external stimuli in physical and biological settings has emerged as exceedingly crucial in recent years. The exceptional electrical conductivity and high surface area of MXenes have significantly accelerated the advancement of flexible sensor research. Recently, MXenes have been integrated into electrospun nanofiber structures, with researchers exploiting these frameworks for a diverse range of applications. This article provides an overview of the latest developments in MXene-functionalized flexible electrospun sensors. Initially, we examined the various flexible sensing mechanisms (such as piezoelectric/resistive, chemoresistive, etc.), followed by an analysis of the numerous factors that impact the electrospinning of MXene-based composites. Subsequently, we highlight the recent areas of application for MXene-functionalized flexible electrospun sensors, encompassing uses from wearable health monitoring to gas detection. Finally, we conclude by delineating the existing limitations and suggesting future research directions for this technology.

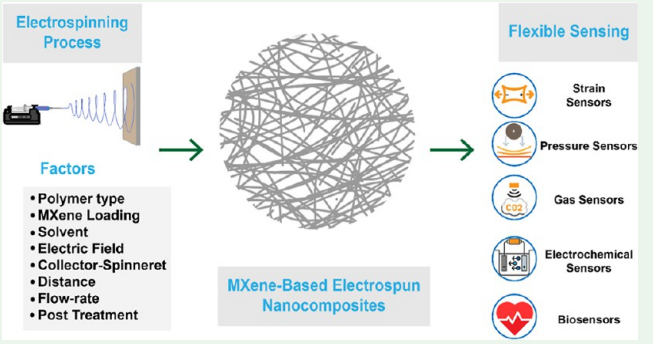

KEYWORDS: *MXene composites, 2D MXene, flexible sensors, electrospinning, nanofibers*

1. INTRODUCTION

The rapid development of flexible and wearable electronics demands high-performance materials with superior properties, including high electrical conductivity, mechanical flexibility, and chemical stability.[1−5] Among the many different functional materials, MXenes, a family of two-dimensional (2D) transition metal carbides, nitrides, and carbonitrides, have attracted significant interest owing to their outstanding properties.[6] Synthesized by a selective etching process from the precursor, MAX phases, MXenes were first isolated in 2011 and are composed of metallically conductive transition metal carbides or nitrides with multifunctional surface chemistry.[7] The high surface area, combined with outstanding mechanical flexibility and record-breaking conductivity, enables MXenes to be implemented in diverse applications, including energy storage,[8−11] electromagnetic interference shielding (EMI),[5,12] and, most importantly, in active/passive flexible sensing.[13,14] In addition to these, the unique surface chemistry of MXenes allows them more suitable to be used for many purposes.[15] MXenes show excellent flexibility and high electrical conductivity,[16] which enables them to be dispersed in organic/polar solvents and can be readily mixed with a large number of polymeric materials.[17] All these unique attributes of MXenes propagate the continuous development in this novel yet rapidly developing field of flexible and wearable sensor technologies.

MXenes can drive the continuous advancement of flexible sensor technologies. Their intrinsic properties, including high electrical conductivity, tunable surface terminations (−OH, −O, −F), excellent mechanical flexibility, hydrophilicity, and large surface area, make them ideal candidates for multifunctional nanocomposite integration.[18] These features facilitate seamless interfacing with electrospun polymer matrices, enabling enhanced charge transport, signal sensitivity, and mechanical compliance in wearable sensor platforms. Moreover, they have a versatile surface chemistry that allows further advanced functionalization and hybridization with other nanomaterials, opening new pathways for tailored sensing mechanisms (e.g., piezoresistive, capacitive, or strain-based responses).[19] The expanding collection of MXene compositions (e.g., Ti_3C_2,

Received: May 26, 2025
Revised: August 6, 2025
Accepted: August 7, 2025
Published: August 13, 2025

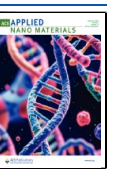

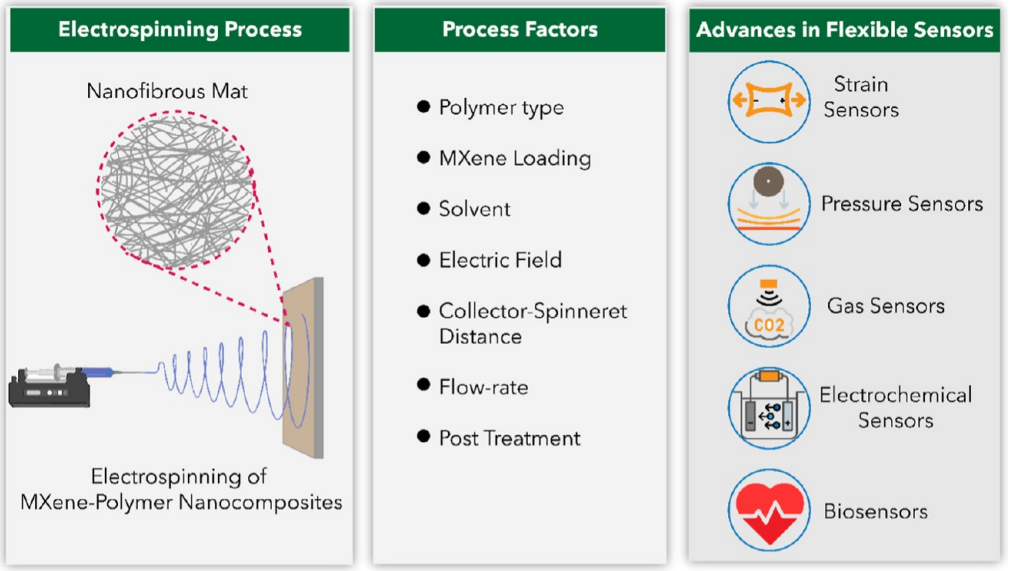

Figure 1. A scheme depicting the synopsis of the review.

Nb_2C, Mo_2TiC_2) and their compatibility with solution processing continue to inspire novel architectures and scalable fabrication strategies.[20] Thus, MXenes not only fulfill current performance requirements but also provides a dynamic and adaptable platform that actively fuels the next generation of flexible and wearable sensing technologies.

Among the variety of methods for fabricating sensor platforms, electrospinning, an extremely versatile and scalable technique, is attracting growing concern for the fabrication of continuous nanofibrous electrodes.[21] Via this technique, a high voltage is applied to a polymer solution to produce fine jets, which solidify to nanofibers collected on a high-speed rotating drum.[22] These electrospun nanofibers have large surface-to-volume ratios, porosities, and high mechanical properties, which are essential for flexible sensing applications.[21,23] When MXenes are implemented into electrospun fibers, the developed nanocomposite inherits the unique features of each counterpart.[24] Such a synergistic combination gives these nanofibers high sensitivity, mechanical strength, and flexibility suitable for flexible sensing applications.[25] The MXene functionalized flexible electrospun sensor interfaces can detect a wide range of stimuli, including mechanical strain,[26] pressure,[27] temperature[28] and a wide variety of chemical species.[29] In addition, they are versatile enough to be used for health monitoring, environmental sensing, and many more.[30]

Compared to other fabrication methods, electrospinning offers a unique combination of scalability, low cost, and compatibility with flexible substrates. While three-dimensional (3D) printing provides high spatial control and design complexity, it often lacks nanoscale resolution and is limited by material viscosity and printhead precision.[31,32] Dip coating has been cost-effective and simple, but results in poor control over film thickness and uniformity, particularly on nonplanar surfaces. Layer-by-layer (L-*b*-L) assembly allows fine-tuning of film thickness and composition, but is time-consuming and difficult to scale up. In contrast, electrospinning enables continuous production of nanofibrous mats with high surface area and tunable morphology, making it highly suitable for conformal coating of flexible and wearable devices. Furthermore, electrospinning setups are relatively low-cost and adaptable to roll-to-roll manufacturing, offering a practical pathway for large-scale integration. This comparative evaluation supports the strategic choice of electrospinning for developing MXene-based flexible sensors.

Owing to this recent surge in flexible sensor research, several reviews have been published in recent years to provide a perspective on electrospun flexible sensing systems. For instance, in early 2024, Mercante et al.[33] emphasized conductive and flexible electrospun micro/nanofiber interfaces for flexible electronics and highlighted their prospective applications in electromagnetic shielding, sensing, and energy storage.[33] A review by Li et al.[34] in 2023 highlighted MXene-based fibers and their diverse applications in flexible and wearable electronics.[34] In another review, Chen et al.[17] focused on the potential and biomedical sensing applications of MXene-based wearable technology.[17] In addition, the potential of MXene-functionalized electrospun nanofibers to improve the functionality of electrochemical devices, including actuators, batteries, fuel cells, sensors, and supercapacitors, was recently summarized in Khademolqorani et al.'s review.[35] The existing literature reviews focus on the present advancements in wearable electronics, yet fail to provide a succinct discussion on MXene-functionalized flexible electrospun sensors. Therefore, there is a critical need to document, examine, and classify the research developments in the fast-evolving area of electrospun MXene-based flexible sensors.

While there exist numerous reviews focusing on various flexible sensor technologies, to the best of the authors knowledge, there is no report on addressing the current state-of-the-art of MXene functionalized flexible electrospun sensors. The present review aims to critically evaluate the recent advancements in flexible sensors based on electrospun MXene materials. Our initial focus will be on summarizing the diverse sensing mechanisms employed. To create flexible sensors integrated with MXene, we will conduct a detailed analysis of the electrospinning process for MXene/polymer composites, exploring synthesis parameters, functionalization techniques, and optimization strategies to enhance nanofiber properties. Furthermore, we will explore the functionality of such flexible sensors across different applications, highlighting their benefits

https://doi.org/10.1021/acsanm.5c02646
ACS Appl. Nano Mater. 2025, 8, 16231−16259

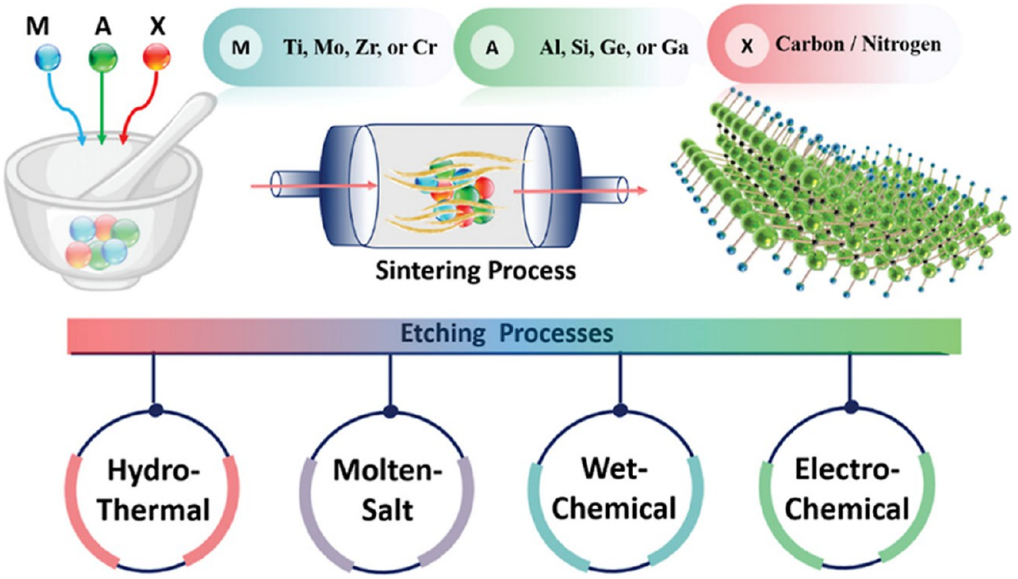

Figure 2. Scheme depicting the etching processes for MXene synthesis. Reprinted with permission from ref 35 Copyright 2023 Wiley-VCH GmbH.

while also scrutinizing any evident limitations. It also aims to provide insights into future directions and opportunities for innovation in MXene functionalized flexible and wearable sensor technologies. Figure 1 depicts the summary of the review.

2. STRUCTURE, SYNTHESIS, AND DELAMINATION OF MXENES

MXenes are a family of 2D inorganic compounds consisting of carbides, nitrides and carbonitrides of transition metals in the periodic table. In order to synthesize MXenes, a layer of MAX phase precursors is eliminated using a chemical etching protocol.[36] MAX phase is represented by its common formula of $M_{n+1}AX_n$, where "M" denotes transition elements (i.e., Sc, Y, Ta, Hf, Cr, V, Ti, Mo, Zr), "A" represents an element from group 13 (IIIA) or 14 (IVA) (i.e., Si, Al, Ge), and "X" is either carbon (C) or nitrogen (N). The value of n can be 1, 2, 3, or 4.[37] The precursor MAX phase has a hexagonal structure where M and X elements are positioned in an octahedral manner.[36] In early studies, MXenes were synthesized from Ti_2AlC, Ti_3AlC_2, V_2AlC, and Nb_2AlC MAX phases.[38] After the removal of A-layer, the resultant MXenes have a common formula of $M_{n+1}X_nT_x$, where T_x is depicted as a wide range of surface termination groups (−Cl, −S, −Se, −OH, −F, −O, etc.).[39] Owing to its comparatively facile processing, $Ti_3C_2T_x$ MXenes are the most widely synthesized MXenes to date.[37] Other MXenes, such as Nb, Mo, and V-based MXenes, are also gaining popularity in recent years.[40]

For synthesizing MXenes, several techniques are prevalent in the literature. Wet chemical, hydrothermal, electrochemical, and molten salt etching are widely utilized protocols for MXene synthesis (Figure 2).[41] The wet chemical method is the most scrutinized route for MXene synthesis. For instance, the first MXene, $Ti_3C_2T_x$, was isolated using 50% HF and Ti_3AlC_2 as MAX phase.[42] Since then, other MXenes such as $Hf_3C_2T_x$, Ti_3CNT_x, Ti_2CT_x, etc. have been synthesized using the HF etching method.[43] However, owing to the safety concerns and toxicity, currently, in situ HF route (minimally intensive layer delamination-MILD) using LiF and concentrated HCl is gaining significant popularity.[44] Apart from the wet chemical method, the electrochemical etching process involves an anode, a cathode, and a DC bias to drive the etching process. Many works have demonstrated the implementation of electrolytes such as HCl, NaCl, HF, etc., to electrochemically etch MAX phase. Using such a route, Ti_2CT_x, a fluorine-free MXene for the first time, was successfully synthesized.[45] Despite its straightforward nature, the electrochemical process could overetch the MAX phase, which can disrupt the structure of MXenes.

In hydrothermal synthesis, MXenes are synthesized by reacting MAX phases with alkali metal hydroxides (i.e., NaOH, KOH) at elevated temperature and pressure. Compared to the wet chemical route, this method is scalable and does not require toxic HF. For instance, monolayer $Ti_3C_2(OH)_2$ was synthesized using KOH at 180 °C for 24 h in an autoclave.[46] Despite its scalable nature, the time and high temperature−pressure requirements restrict its use for large-scale synthesis. Lastly, the Lewis acid-mediated molten salt route is leveraged to isolate MXenes from nonconventional MAX phases. Using such route, −Cl terminated MXenes such as, $Ti_3C_2Cl_2$ and Ti_2CCl_2 were isolated in 2019.[47] In addition, MXenes without surface termination groups and with terminal groups can be engineered using the molten salt route, as reported by Kamysbayev et al.'s study.[48] Hence, the molten salt route provides more options for diverse MXene applications by tuning the surface chemistry.

After the etching process, the resultant multilayered MXenes are held together by weak van der Waals and hydrogen bonding interactions. To achieve mono to few-layer MXene sheets, mechanical delamination or intercalation between nanosheets is required. While mechanical delamination provides a low yield, the intercalation process can further weaken the interlayer bonds and help in the facile delamination process. To date, organic compounds (i.e., $N_2H_4{\cdot}H_2O$, *N*,*N*-dimethylformamide (DMF)),[49] molecules (i.e., dimethyl sulfoxide (DMSO), water),[50] and cations (i.e., Li^+, H^+, Al^{3+}, etc.)[51] are the widely utilized intercalants for MXene delamination. In principle, the delamination and intercalation rely on the type of etchant utilized, the intercalating agent, and the sonication time. More sonication time leads to low yield and more structural defects.[52]

Despite such progress in synthesis techniques, there remain some drawbacks for Ti-based MXenes. The inability to control surface termination groups and instability due to oxidation are

https://doi.org/10.1021/acsanm.5c02646
ACS Appl. Nano Mater. 2025, 8, 16231−16259

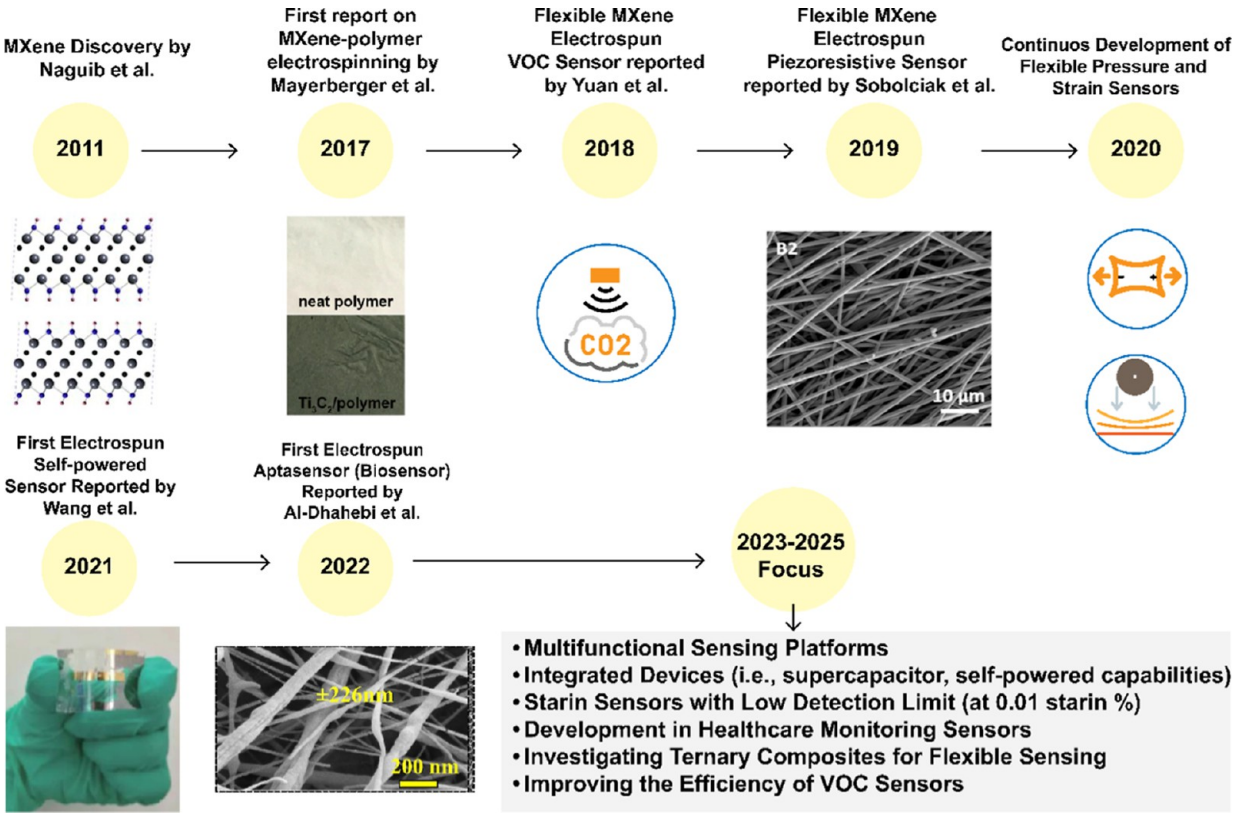

Figure 3. Historical development of MXene-based electrospun composites for flexible and wearable sensing applications. Reprinted with permission from ref 42 Copyright 2011 Wiley-VCH. Reprinted with permission from ref 55 Copyright 2017 Wiley Periodicals, Inc. Reprinted with permission from ref 56 Copyright 2019 MDPI. Reprinted with permission from ref 57 Copyright 2021 Springer. Reprinted with permission from ref 58 Copyright 2022 Elsevier Ltd.

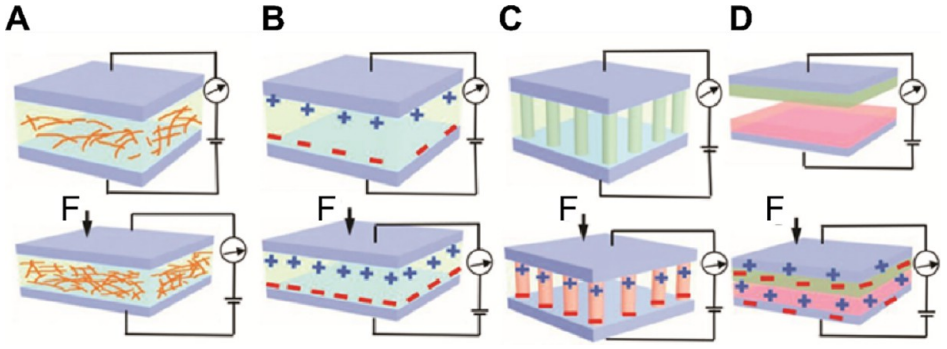

Figure 4. Scheme depicting various sensing mechanisms. (A) Piezoresistive, (B) capacitive, (C) piezoelectric, and (D) triboelectric sensing mechanisms. Reprinted with permission from ref 86 Copyright 2021 Wiley-VCH GmbH.

some of the prevalent problems for MXenes.[53] Besides, the smaller flakes tend to oxidize faster and have less stability compared to larger flakes. Several strategies have been realized to increase the stability of MXenes. Surface modification strategies such as polyanionic salt-assisted edge-capping, removal of oxygen from MXene colloidal solutions, and dispersing in organic solvents are some of the key ways to increase MXene stability and prevent oxidation.[18,54]

3. FLEXIBLE SENSING WITH MXENES

Since the isolation of MXene by Naguib et al.,[42] the application of MXene-based composites has expanded. Figure 3 summarizes the historical development of MXene-based electrospun composites and their applications in flexible and wearable sensing. This chapter will critically discuss the sensing mechanisms of MXene-based polymer composites. Key mechanisms such as piezoresistive, capacitive, piezoelectric, triboelectric, and chemiresistive sensing principles are discussed.

3.1. Piezoresistive Sensing. The piezoresistive mechanism functions by the resistive strain effect, which alters the resistance or current of the sensing electrode under any mechanical stimuli (bending, compression, etc.). When mechanical deformation occurs, the contact area and the density of the sensing electrode are changed. As a result, the resistance of the sensing electrode is changed, which provides a distinguishable electrical signal for analysis. In principle, the resistance change $(\frac{\nabla R}{R})$ can be calculated using eq 1.[59]

https://doi.org/10.1021/acsanm.5c02646
ACS Appl. Nano Mater. 2025, 8, 16231−16259

$$\frac{\nabla R}{R} = \frac{\nabla \rho}{\rho} + (1 + 2\nu)\varepsilon \quad (1)$$

where ρ is the resistivity, ν is the Poisson's ratio, and ε is the applied mechanical strain on the sensor electrode.

The piezoresistive mechanism is predominantly utilized in flexible MXene-based physical sensors. To date, the piezoresistive mechanism has been leveraged to fabricate electrospun MXene-based flexible strain[60] and pressure sensors.[61] Here, the electrospun MXene polymer composite acts as the conductor/sensing electrode. When mechanical strain is applied, the electrical resistance of the nanocomposite changes and gives electrical signals (Figure 4A). While the polymer provides the mechanical resistance to deformation, the 2D MXene nanosheets contribute to the overall electrical conductivity. Owing to mechanical deformation, such as stretching or compression conditions, the nanosheets slide over each other, and the relative interlayer distance between nanosheets is increased (if stretched) or decreased (if compressed). For this reason, the resistance is changed and a distinguishable electrical signal is generated, which responds to the magnitude of mechanical strain applied.[62,63] By monitoring these resistance fluctuations, MXene-based piezoresistive sensors can sense and quantify various mechanical stimulations, such as strain, pressure, or touch.[64,65]

Under increasing mechanical strain or pressure, the MXene nanosheets and electrospun fibers undergo gradual realignment and densification, leading to nonuniform changes in conductive pathways. This causes the resistance to change disproportionately with applied force. At low strains, initial deformation primarily affects intersheet contact resistance, whereas at higher strains, the breakdown or reformation of conductive networks dominates the response. This shift in dominant conduction mechanism leads to nonlinearity. The resistance at nanoscale gaps between MXene sheets may follow quantum tunneling behavior, which is inherently nonlinear with respect to the separation distance under strain. The polymer matrix in electrospun composites often exhibits viscoelastic properties. This mechanism explains the time-dependent strain recovery and hysteresis, further contributing to nonlinear electrical behavior during loading−unloading cycles.[64−68]

Electrospun MXene-based flexible piezoresistive sensors offer high sensitivity, large mechanical strain, and excellent flexibility. However, the piezoresistive response of MXene-based flexible sensors may be nonlinear, posing challenges in accurately detecting mechanical deformations. Additionally, the flexible MXene-integrated piezoresistive sensors offer limited dynamic range, which significantly hinders their capacity to analyze a wide spectrum of mechanical deformations.[69,70]

3.2. Capacitive Sensing. The capacitive sensing mechanism functions by converting the applied pressure changes into a capacitance change. The capacitive sensors consist of two top and bottom electrodes with a dielectric layer in between. When any mechanical deformation occurs, the distance between the layers is changed, which results in a change in capacitance (Figure 4B). The capacitance (C) can be calculated using eq 2.[71]

$$C = \frac{\epsilon_r \epsilon_0 A}{D} \quad (2)$$

where ϵ_r is the dielectric constant, ϵ_0 is the relative dielectric constant, A is the effective contact area and D is the distance between the two electrodes. In principle, capacitive sensors are constructed in a parallel electrode configuration. In terms of flexible sensing, the effective geometry variation between electrodes during deformation causes low sensitivity.

MXenes possess abundant surface terminations and high surface area, which make their dielectric environment highly sensitive to minor external perturbations, such as environmental humidity, temperature fluctuations, or airborne contaminants. These can induce unintentional variations in capacitance. The flexible nature of electrospun substrates can lead to microscopic variations in electrode−dielectric spacing during motion or deformation, resulting in unstable capacitance readings and increased signal noise. Due to their high conductivity and 2D structure, MXenes can act as antennas for ambient electromagnetic fields, which may induce parasitic currents or noise in the capacitive readout. Imperfect electrical contacts or fluctuating interface resistance in flexible configurations can be coupled with parasitic capacitance in the measurement circuit, amplifying background noise.[72−75]

In recent years, flexible MXene-based capacitive sensor composites have been implemented as electronic skin (e-skin),[76] pressure sensing,[77] and physiological monitoring applications. Typically, MXene-based electrospun composites are leveraged as a dielectric layer to enhance the sensor's performance. For instance, Zhang et al.[77] designed a thermoplastic polyurethane (TPU)/diazotization-modified $Ti_3C_2T_x$ nanocomposite film for capacitive pressure sensors. The dielectric composite achieved a high dielectric constant of 817, and the assembled capacitive pressure sensor showed a sensitivity of 10.2 kPa^{-1} at a pressure range of 0−8.6 kPa. Such sensitivity could be attributed to a large dielectric change for a constant deformation, which enhances the sensitivity of flexible sensors. Despite such attributes, MXene-based flexible capacitive sensors are prone to noise interference, which impacts their operational efficiency. Additionally, these sensors exhibit a constrained dynamic range that limits their capacity to gauge a broad spectrum of mechanical stimuli.

3.3. Piezoelectric Sensing. Piezoelectric sensing is based on a unique effect shown by piezoelectric materials. The piezoelectric effect refers to the generation of electricity upon applied mechanical strain. Such phenomena occur owing to the force-induced polarization within the material. The charge is nullified when the mechanical force is removed (Figure 4C). The polarization of the electric charge alters when the mechanical force direction is changed. The generated charge can be amplified and transformed into an electrical signal that is proportional to the applied force. The flexibility (S) and the charge density (D) of the process in a piezoelectric material can be calculated using eqs 3 and 4.[78]

$$S = s^E T + \mathrm{d}E \quad (3)$$

$$D = \mathrm{d}T + \epsilon E \quad (4)$$

where s is the applied mechanical strain, T is the stress, E is the electric field intensity owing to the piezoelectric effect. Compared to triboelectric sensing, the piezoelectric mechanism is efficient in converting mechanical energy into electrical energy. However, traditional piezoelectric materials are brittle (i.e., ceramics) and have low output efficiency. Hence, designing composite materials with enhanced mechanical attributes is crucial in designing high-performance piezoelectric sensors.

The high conductivity of MXenes and their sharp dielectric contrast with insulating polymers lead to strong Maxwell−Wagner−Sillars (MWS) interfacial polarization under an external field, increasing the effective dielectric constant.

https://doi.org/10.1021/acsanm.5c02646
ACS Appl. Nano Mater. 2025, 8, 16231−16259

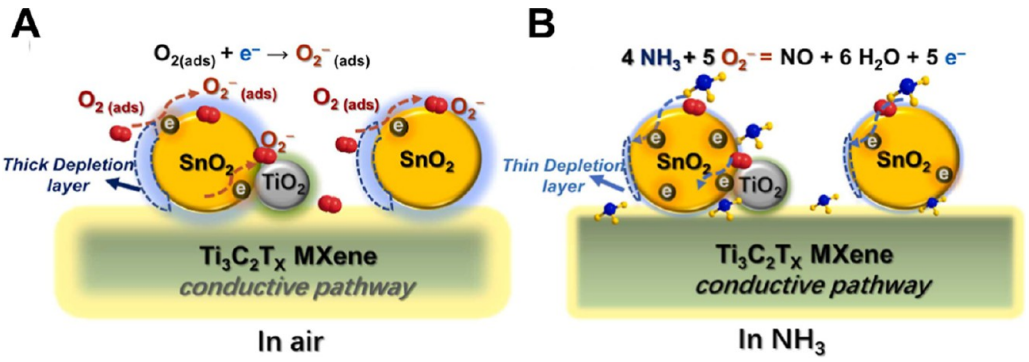

Figure 5. Chemiresistive sensing mechanism of MXene-based composites for NH_3 detection. (A) Interaction with air. (B) Interaction with NH_3. Reprinted with permission from ref 91 Copyright 2023 Elsevier B.V.

MXenes provide abundant surface terminations (−OH, −F, −O), which facilitate localized charge trapping and accumulation at the polymer-MXene interface, thereby increasing surface charge density. The 2D nature of MXenes promotes fast charge transport pathways, contributing to enhanced space charge accumulation and dielectric response within the composite.[79−81]

To design efficient piezoelectric materials, MXenes and their composites are now widely investigated. MXenes can show a piezoelectric effect owing to their noncentrosymmetric lattice structure. In a study conducted by Tan et al.[82] reported that monolayer $Ti_3C_2T_x$ MXene generates stable piezoelectric voltage under dynamic strain conditions with a conversion efficiency of 11.5%.[82] Besides, surface engineering of 2D MXenes enables them to be tuned to a noncentrosymmetric polyatomic structure conducive to the enhanced piezoelectric effect.[83] As a result, when MXenes are implemented within polymer composites, they synergistically increase the overall conductivity and are conducive to enhancing the electric polarization to improve the voltage output of the composite. MXene-based electrospun flexible sensors can be self-powered, generating electrical energy through mechanical action, making them suitable for energy-harvesting applications.[83] Besides, MXene-based flexible piezoelectric sensors have the capability to quickly respond to variations in mechanical stimuli, allowing real-time monitoring and detection.[84] Despite this, the piezoelectric coefficient of MXene-based flexible nanocomposites is relatively small, which impedes their capacity to generate detectable electrical signals. Moreover, the piezoelectric sensitivity is greatly governed by factors such as the orientation of MXene nanosheets, flake size, surface termination, and the interactions within the composite matrix, posing considerable challenges in achieving consistent piezoelectric performance.[85]

3.4. Triboelectric Sensing. Triboelectric sensors depend on the generation of an electrical charge due to the contact and separation between two different materials, known as the triboelectric effect (Figure 4D). Like capacitive sensing, triboelectric sensors are composed of a two-electrode configuration. For triboelectric sensing, two different electrode materials are leveraged, where the electrodes generate charge upon contact and separation. The charge variation generates an electrical signal (voltage or current) that can be utilized to detect mechanical stimuli such as pressure or vibration. The voltage output (V) can be calculated using eq 5.[87]

$$V = -\frac{Q}{C} + V_{OC} \tag{5}$$

where Q is the charge transfer quantity, C is the capacitance between two layers, and V_{OC} is the voltage generated by friction charge polarization. However, the surface wear can lead to poor and unstable performance. Hence, investigating new materials for triboelectric sensing is crucial.

To develop high-performance self-powered sensors, MXene-based electrospun composites have been investigated recently. The high electronegativity of the MXene surface and the mechanical flexibility of MXenes allow their use in flexible triboelectricity-directed self-powered sensors. MXenes are typically fabricated as a highly electronegative composite tribolayer in flexible self-powered sensors since the integration of MXenes in polymers enhances the surface charge density and dielectric constant. For instance, Bhatta et al.[88] incorporated MXene nanosheets within PVDF nanofibers, which increased the surface charge density of the composite by 80% and boosted the dielectric constant by 270%. Additionally, triboelectric sensing can be used to detect a wide range of mechanical stimuli, including pressure, touch, and motion. However, MXene-based flexible triboelectric sensors often exhibit low sensitivity, which can limit their ability to detect small changes in mechanical stimuli. Furthermore, these sensors can be susceptible to noise interference, which can affect their performance.

3.5. Chemiresistive Sensing. Chemiresistive sensors are constructed by employing a sensing material deposited onto a substrate, which is connected to detection instruments to measure any change in the sensing material. The function of such a sensor is to detect fluctuations in the electrical resistivity of the sensing material while in an environment filled with target analytes. The performance of chemiresistors is analyzed by testing the selectivity, sensitivity, and stability of the sensing material in a contaminated environment. For flexible chemiresistive sensors, researchers investigate key features such as sensing layer thickness, material fabrication, flexibility, self-operation, and sensor electrode design.[89]

To design chemiresistive sensing platforms, low-dimensional materials with high surface area, mechanical flexibility, and high conductivity are desired. MXenes are gaining considerable attention for chemiresistive sensing owing to their high surface area, electrical conductivity, and surface functional group tunability. The high surface area and the presence of tunable functional groups on MXene-based electrospun composite surfaces make them highly sensitive to the presence of gases, vapors, or bioanalytes.[90] Typically, the chemical species is adsorbed on the surface terminations of MXene-based composites, which generates a detectable electrical signal. For example, Yu et al.[91] explored the chemiresistive sensing

https://doi.org/10.1021/acsanm.5c02646
ACS Appl. Nano Mater. 2025, 8, 16231−16259

Table 1. Summary of Key Sensing Mechanisms

sensing mechanism	measured parameter	stimuli type	benefits	limitations	application area	references
piezoresistive	electrical resistance	pressure, bending, and stretching	low-cost and easy to fabricate	delayed response	healthcare monitoring, E-skins, and human-machine interactions	92,93
capacitive	capacitance	pressure, touch, or strain	low power requirement	geometry-dependent and small response range	soft robotics, E-skins, healthcare monitoring	94,95
piezoelectric	generating electric charge/voltage	pressure, force, vibration, and bending	self-powered capability	low power output	self-powered sensor, structural health monitoring, energy harvesting	96,97
triboelectric	generating electric charge/voltage	friction, rubbing, vibration, impact, pressure, and bending	self-powered capability	surface wear	self-powered sensor, vibration and impact sensing, soft robotics	98,99
chemiresistive	electrical resistance	chemical species (liquid/gas)	low-cost and small form factor	low selectivity and environment-dependent	gas sensing, environmental monitoring	89,100,101

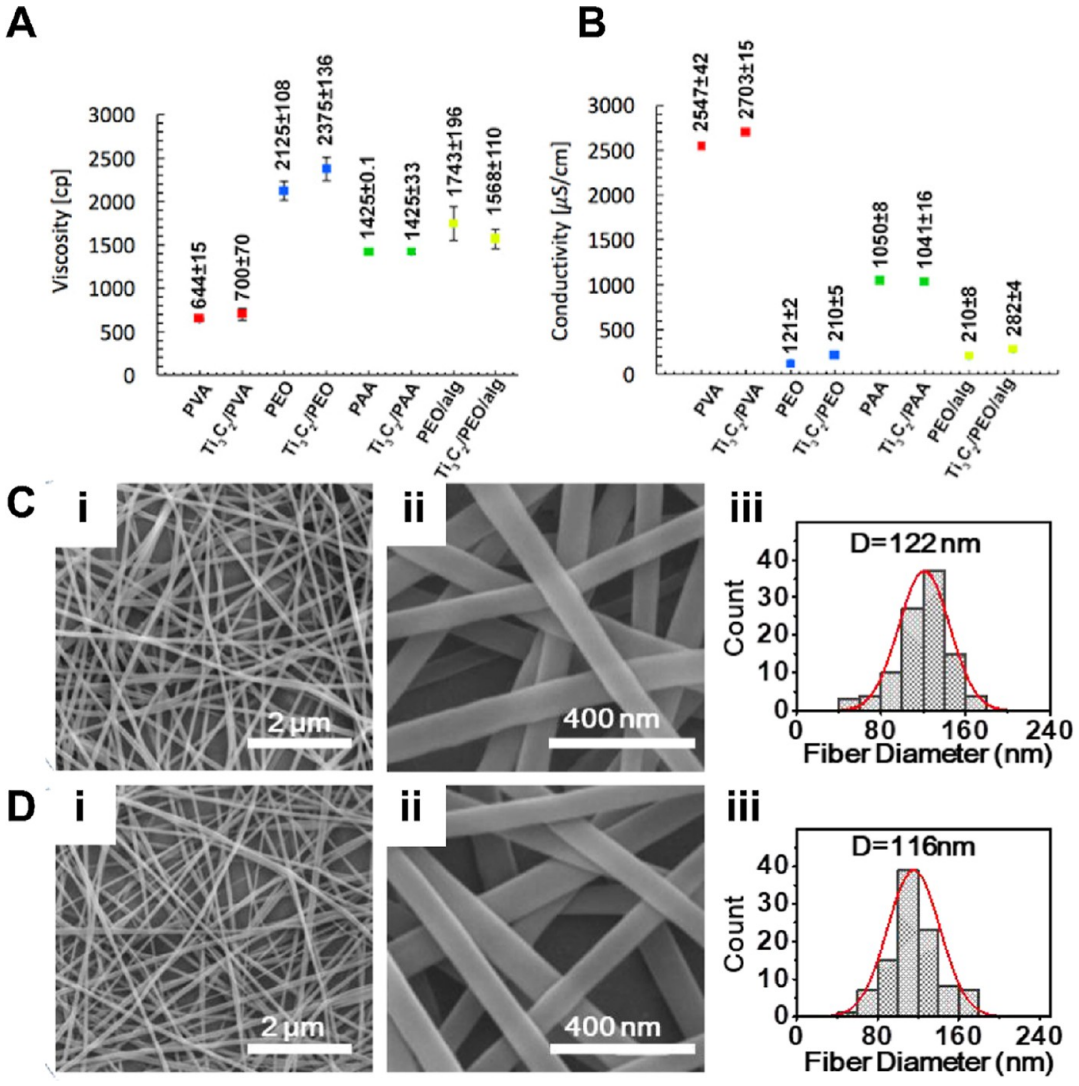

Figure 6. (A) Viscosity comparison of pristine polymer and MXene-loaded polymer solutions. (B) Conductivity comparison of pristine polymer and MXene-loaded polymer solutions. Reprinted with permission from ref 55 Copyright 2017 Wiley Periodicals, Inc. (C) (i–iii) SEM images and diameter distribution of P@M-1 nanofibers. (D) (i–iii) SEM images and diameter distribution of P@M-2 nanofibers. Reprinted with permission from ref 109 Copyright 2019 Elsevier B.V.

mechanism of $Ti_3C_2T_x$–SnO_2 composite for NH_3 sensing and reported that the composite showed high selectivity in air and NH_3 environment (Figure 5A,B). When NH_3 molecules were adsorbed onto the oxygen of SnO_2, the Schottky barrier was reduced between $Ti_3C_2T_x$ and SnO_2. As a result, a decrease in the channel resistance was observed and detected for analysis.[91]

Chemiresistive sensors utilizing MXene-based composites demonstrate high sensitivity to specific chemical species, allowing precise detection and monitoring for volatile organic compounds (VOCs), environmental monitoring, and wearable electronics. Moreover, their tunable surface terminations allow these sensors to identify a wide range of chemical analytes.

https://doi.org/10.1021/acsanm.5c02646
ACS Appl. Nano Mater. 2025, 8, 16231–16259

However, challenges arise due to oxidation in a humid environment, which renders these composites with a low service time. Table 1 shows the comparison and application areas of sensing mechanisms.

4. ELECTROSPINNING OF MXENE FUNCTIONALIZED NANOFIBERS

A polymer solution must be prepared for electrospinning MXene-polymer composites. After which MXenes are dispersed into the polymer solution and sonicated to achieve a homogeneous dispersion. The MXene-polymer solution will then be utilized for electrospinning MXene functionalized composites.[55,102] We will focus on the role of various factors affecting the electrospinning of MXene-functionalized nanofibers. Factors such as polymer selection, MXene loading, solvent selection, and varying electrospinning parameters significantly affect the properties of MXene functionalized electrospun composites.

4.1. Polymer Selection. The type of polymer used has a significant role in governing the morphology of MXene-based electrospun nanocomposites. To date, polyurethane (PU) variants,[103,104] polyvinylidene fluoride (PVDF),[105] poly(vinyl alcohol) (PVA),[106] polyacrylonitrile (PAN),[107] and nylon-6,6[108] have been utilized to fabricate MXene-based electrospun composites for flexible sensing. The polymer used has a critical role in determining not only the viscosity and conductivity of the polymer solution but also the fiber diameter and crystallinity of the electrospun composites. For instance, Mayerberger et al.[55] conducted an in-depth analysis of the effect of polymer type on the fiber morphology of the electrospun MXene-polymer composites. Figure 6A,B depicts the viscosity and conductivity of pristine polymer and MXene-loaded polymer solutions. The group fabricated $Ti_3C_2T_x$/poly(acrylic acid) (PAA), $Ti_3C_2T_x$/poly(ethylene oxide) (PEO), PVA, and $Ti_3C_2T_x$/alginate/PEO via an electrospinning process with a $Ti_3C_2T_x$ loading of 1 wt.%. It was found that $Ti_3C_2T_x$/PEO composite achieved a 20% reduction in fiber diameter (419 to 335 nm), attributed to the increased conductivity (973.6%) and viscosity (11%) of the spinning dope. PVA−$Ti_3C_2T_x$, in contrast, exhibited a limited conductivity increase (6.2%) and an 8.7% rise in viscosity in the spinning dope, resulting in thicker fibers (573−762 nm) due to stronger hydrogen bonding. PAA−$Ti_3C_2T_x$ had minimal viscosity change but a 38.9% fiber diameter reduction (298−182 nm), indicating weaker polymer-MXene interactions and limited solution conductivity. Alginate/PEO−$Ti_3C_2T_x$ saw a 10.1% viscosity drop but a 34.6% conductivity rise in solution conductivity, contributing to fiber uniformity. Such results clearly indicate the need to select the proper polymer to fabricate electrospun MXene/polymer composites.

4.2. MXene Loading. The characteristics and functionality of the resultant nanofibers are significantly influenced by the loading of MXene nanosheets into the polymer solution during electrospinning. It was found that MXene loading can affect the nanostructure, smoothness and diameter distribution of the nanofibers. Gao et al.[109] experimented with PAN-MXene nanofibers and investigated the role of MXene loading on the nanostructures of nanocomposite fibers. The group prepared PAN-$Ti_3C_2T_x$ MXene nanofibers by doping the polymer solution with 0, 25, 50, 100, and 400 μg of MXene and denoted the obtained nanofibers as P@M-1, P@M-2, P@M-3 and P@M-4, respectively. It was found that at small MXene loading (for P@M-1 and P@M-2), the diameter distribution was not significant, had an average diameter of 122 and 116 nm for P@M-1 and P@M-2. Besides, the resultant fibers were smooth and bead-free (Figure 6C,D). However, as the MXene loading increased to 400 μg, the diameter increased to 120 nm (P@M-4), and the diameter distribution was also wider. Additionally, the fibers were not smooth and noticeable beaded structures were found. Such phenomena could be attributed to the aggregation of MXene nanosheets, which increased the roughness and diameter of the nanofibers. This study indicates that engineering MXene-based nanofibers with moderate MXene loading could improve nanofiber structure, while excessive loading could lead to rough nanofibers with inconsistent diameter distribution.

4.3. Solvent Selection. The technique and characteristics of the final nanofibers produced via electrospinning MXene-based nanofibers are significantly influenced by the solvent used. To create a homogeneous solution, the solvent must first successfully dissolve the polymer and disperse MXene nanosheets. While MXenes show relatively low zeta potential (−39.5 to −63 mV) at neutral pH in water, most of the polymers utilized cannot be dissolved in water. To mitigate this issue, a number of polar organic solvents have been introduced to the spinning dope for fabricating electrospun MXene nanocomposites. To date, DMF,[110] acetone,[105] water,[106] formic acid,[111] tetrahydrofuran (THF),[103] and sodium dodecyl sulfate (SDS)[112] have been utilized for preparing electrospinning polymer solutions. In addition, solvents with elevated boiling temperatures and low vapor pressure typically produce greater viscosities and impact jet formation and fiber shape.[113]

The choice of solvent plays a crucial role in determining the conductivity and viscosity of the electrospinning solution, directly affecting jet stability, Taylor cone formation, and fiber alignment. A solvent with higher conductivity (i.e., DMF,[110] THF,[103] etc.) can improve fiber uniformity, while one with optimal viscosity (1425−2375 cP[55]) ensures smooth flow during electrospinning of MXene-based nanofibers.[55] Additionally, the evaporation rate of the solvent significantly impacts MXene-based fiber formation−faster evaporation helps eliminate residual solvent quickly, reducing bead formation and enhancing fiber structure. To achieve a homogeneous dispersion of MXene within the polymer matrix and prevent agglomeration, the solvent must be carefully chosen for its compatibility with MXene suspensions. Beyond processing considerations, safety and environmental impact are equally important. Selecting a solvent with low toxicity, minimal volatility, and reduced hazardous fume emissions helps mitigate health risks and environmental harm, ensuring a safer and more sustainable electrospinning process.[55] Using solvents with low toxicity, minimal volatility, and reduced hazardous fume emissions directly mitigates both occupational health risks and environmental impact. Low-toxicity solvents reduce the likelihood of skin irritation, respiratory issues, or long-term health complications for researchers and workers during handling and processing. Minimal volatility limits the evaporation of harmful vapors into the workspace, lowering the need for aggressive ventilation and decreasing atmospheric emissions. Furthermore, solvents with reduced hazardous fumes are generally easier to contain, recover, and dispose of, aligning with green chemistry principles and regulatory safety standards.

4.4. Electrospinning Parameters. The electrospinning parameters for MXene/polymer composites are meticulously optimized to enhance fiber morphology, electrical conductivity, and mechanical flexibility—critical attributes for flexible sensing applications.[114,115] The electrospinning nozzle gauge, typically

https://doi.org/10.1021/acsanm.5c02646
ACS Appl. Nano Mater. 2025, 8, 16231−16259

Table 2. Summary of Electrospinning Parameters for Fabricating MXene-Functionalized Electrospun Composites

sensor composite	polymer	additives in spinning dope	MXene loading	solvent	spinning nozzle gauge (G)	electric field strength (kV)	distance	flow rate	collector type	relative humidity	temperature	post-treatment	application	reference
TPU-MXene-TPU	TPU		2 mL	DMF/acetone (1:1)	22 G	12 kV	10 cm	1.5 mL/h	aluminum foil		RT	electrostatic spraying of MXene ink, 6 cm distance, 1 mL/h flow rate, roller rpm 60 cm/min, then another TPU layer was electrospun on the MXene sensing layer to achieve the final strain sensor	strain sensing for human motion monitoring	110
MXene-coated-PU	PU			DMF/THF (1:1)		15 kV	20 cm	2 mL/h (6 h)	aluminum foil	25−30%	25 °C	spray-coated MXene onto the PU nanofiber membrane	STrain sensing for physiological signal monitoring	103
MXene-nylon nanoyarns	Nylon-6,6		10−20 mg mL^{-1}	formic acid	21 G	10−20 kV	1−3 cm	0.3−1 mL/h	aqueous MXene solution				energy-storing yarn	108
MXene-PU nanoyarns	PU		10−20 mg mL^{-1}	DMF/THF (70/30)	21 G	10−10 kV	1−3 cm	0.3−1 mL/h	MXene in DMF/water (7/3)				STrain sensing yarns	
TPU/MXene/MWCNT	TPU			DMF/THF (1:1)		15 kV	14 cm	1 mL/h	80 r/min	40 ± 5%	20 ± 2 °C	alternating vacuum filtration of MXene and MWCNT solutions	strain sensing film for human motion monitoring	104
PPy/MXene-PVDF	PVDF			acetone/DMF (2:3)	21 G	18 kV	15 cm	2 mL/h	aluminum foil, 400 rpm	30%	RT	drop casting of PPy and MXene solution onto $FeCl_3$-modified PVDF	finger bending, bicep stretching, and ankle stretching	105
MXene/GnP/CNC-SBS	styrene−butadiene styrene (SBS)			ethanol/IPA (1:2)		15 kV	10 cm	1 mL/h				ultrasonic-assisted atomization and vacuum filtration	can successfully record different body deformations	117
BaTiO3/MXene-PVDF-TrFE	PVDF-TrFE	1 wt % $BaTiO_3$/MXene		DMF/acetone (3:7)	tip diameter-0.8 mm	16 kV	12 cm	1 mL/h	aluminum foil			no post-treatment	electronic skin for human motion detection: finger flex, walking, running, jumping	61
MXene-SF	silk fiber	silk fibrion		formic acid (15% w/v)		1 kV/cm		1 mL/h				dip coating with MXene	E-skin and disease diagnostics	111
MXene/ZIF-67/PAN	PAN			DMF		17 kV	15 cm	0.3 mL/h				drop coating with MXene	urination monitoring by detecting	107

https://doi.org/10.1021/acsanm.5c02646
ACS Appl. Nano Mater. 2025, 8, 16231−16259

Table 2. continued

sensor composite	polymer	additives in spinning dope	MXene loading	solvent	spinning nozzle gauge (G)	electric field strength (kV)	distance	flow rate	collector type	relative humidity	temperature	post-treatment	application	reference
													bladder volume change	
PDMS/MXene-PVA	PVA			water		the positive voltage is 26 kV, the negative voltage is 2.7 kV	17 cm						physiological signal detection and human-machine interactions	106
MXene-PU/PAN/AgNW	PAN + PU			DMF		the positive high voltage was 9 kV, and the negative high voltage was 2 kV	15 cm	0.12 mm/min	aluminum foil 2800 rpm			spray coating with MXene dispersion	the sensor can monitor radial artery, carotid artery, speech, and so on	57
MXene/PVA-MoSe2	PVA			water		18 kV	15 cm	0.3 mL/h		11−97% RH	25 °C		can harvest energy from human motion and detect humidity	57
PVA/MXene/TiO2-CA	PVA			water		24 kV	15 cm	0.2 μL/s	aluminum foil			dip coated with TiO_2 nanoparticles	self-powered ammonia sensing	116
PVA/MXene/TiO2-CA	cellulose acetate			Acetone/DMF- 2/1		17 kV	15 cm	0.7 μL/s	aluminum foil			dip coated with TiO_2 nanoparticles	intelligent NH_3 sensing harvesting human motion	116
PVA/PEI/MXene	PVA/PEI (3:1)			DI water with SDS		15 kV	14 cm	0.3 mL/h				MXene was dip-coated onto the fabricated nanofibers	VOC detection (methanol, ethanol, acetone, etc.)	112

https://doi.org/10.1021/acsanm.5c02646
ACS Appl. Nano Mater. 2025, 8, 16231−16259

ranging from 21 to 22 G, is carefully selected to ensure uniform fiber formation while maintaining a stable jet ejection for polymer solutions incorporating MXene nanosheets. The electric field strength, which varies between 10 kV and 26 kV, plays a crucial role in forming continuous fibers with minimal bead defects.[57,116] Higher voltages (>20 kV) promote extensive fiber stretching, resulting in finer nanofibers with enhanced electrical conductivity, which are particularly advantageous for strain and pressure sensing applications. In contrast, moderate voltages (∼15 kV) contribute to maintaining uniform fiber thickness, ensuring consistent performance across various sensing applications.[106]

The tip-to-collector distance, typically set between 10 and 20 cm, is carefully controlled to optimize solvent evaporation and fiber deposition. A shorter distance (∼10 cm) facilitates rapid deposition, which is beneficial for the formation of thicker sensing layers, whereas a longer distance (∼20 cm) allows for improved solvent evaporation, minimizing structural defects that may compromise electrical performance in wearable or stretchable sensors.[107,111] Similarly, the flow rate, which ranges from 0.2 μL/s to 2 mL/h, is a determining factor in fiber diameter and porosity, both of which directly impact the sensitivity and response time of MXene-based composite flexible sensors.[108] Lower flow rates (∼0.2−0.3 μL/s) facilitate the formation of ultrafine, highly porous nanofibers suitable for capacitive and resistive sensing, while higher flow rates (∼2 mL/h) contribute to the development of uniform conductive networks, which are ideal for strain and humidity sensing applications.[104]

The collector type significantly influences fiber orientation and mechanical flexibility, both of which are essential for sensors that experience mechanical deformations such as bending and stretching. Stationary aluminum foil is commonly utilized to achieve random fiber deposition, promoting isotropic electrical conductivity, whereas rotating drum collectors (400−2800 rpm) induce fiber alignment, which is particularly beneficial for anisotropic strain sensors requiring directional conductivity.[103,104] Additionally, the relative humidity (RH), which varies from 30% to 97% RH, plays a crucial role in determining fiber morphology. Controlled humidity levels below 40% contribute to the formation of smooth, uniform fibers with stable electrical properties, whereas elevated humidity levels (>90%) introduce nanoporosity, thereby enhancing sensor sensitivity, particularly in humidity and gas sensing applications.[107,110] Lastly, the temperature, generally maintained at room temperature (RT) or 25 °C, ensures consistent solvent evaporation, mitigating phase separation effects that could otherwise degrade the mechanical and electrical properties of the sensing material.[57]

By systematically tuning these electrospinning parameters, MXene functionalized electrospun composites can achieve superior electrical conductivity, mechanical flexibility, and environmental stability, making them highly suitable for advanced flexible sensing applications, including wearable electronics, human motion detection, and environmental monitoring. Table 2 provides a detailed overview of the electrospinning process for fabricating MXene-functionalized electrospun composites.

5. MXENE FUNCTIONALIZED ELECTROSPUN SENSORS

In recent years, flexible sensors have gained tremendous popularity owing to the recent progress in wearable and portable technology.[118] The unique surface chemistry of MXene allows it to be an excellent reinforcing material for nanofiber spinning, and such a nanocomposite electrode acts as an effective interface for flexible sensing applications. MXene-based flexible electrospun sensors are being investigated in various settings and applications, including piezoresistive,[119] strain,[120] self-powered,[116,121] biomonitoring,[112] and as optical sensors.[122] The ability of MXene-functionalized electrospun sensors to detect a broad range of stimuli stems from the synergistic integration of two key material systems: (1) the high surface area, electrical conductivity, and tunable surface terminations of MXenes, and (2) the porous, flexible, and mechanically adaptive nature of electrospun fiber networks.[123] MXenes provide a highly conductive and responsive sensing layer that can effectively transduce mechanical, thermal, or chemical signals into electrical outputs. Their surface functionalities (e.g., −OH, −F, −O) allow for selective interaction with environmental species, enabling sensitivity to humidity, gases, or biomolecules. Meanwhile, electrospun fibers enhance the mechanical deformability and surface-to-volume ratio of the composite, allowing the sensor to respond efficiently to pressure, strain, and temperature fluctuations.[124,125] Together, this hybrid interface supports multiple sensing mechanisms, including piezoresistive, capacitive, and chemiresistive responses, making the platform inherently multimodal and capable of detecting a variety of physical, chemical, and biological stimuli.[126]

MXene-based electrospun sensors can be functionalized through multiple strategies to enhance their performance and tailor them for specific sensing applications. One common method is surface functionalization, where functional groups such as $-NH_2$, −COOH, or −SH are introduced onto MXene surfaces to improve selectivity and chemical interactions. Polymer blending is another approach, where MXenes are incorporated into electrospinnable polymers (e.g., PVDF, PEO) to modulate electrical and mechanical properties. Nanoparticle decoration involves attaching metal or metal oxide nanoparticles (e.g., Ag, Au, ZnO) to enhance sensitivity or add catalytic functionality. L-*b*-l assembly allows construction of multilayer architectures with alternating materials, optimizing charge transport and sensor stability. Lastly, doping or cross-linking agents can be used within the polymer matrix to adjust conductivity and sensing behavior. These diverse functionalization pathways make MXene-based electrospun sensors highly versatile platforms for detecting physical, chemical, and biological stimuli.[127−130] This chapter will summarize the recent state-of-the-art MXene-integrated flexible electrospun sensors in these diverse applications and evaluate their performance parameters in such settings.

5.1. Strain Sensors. MXene-based strain sensors are thoroughly investigated and used in numerous applications, including automation, human-machine interface, health monitoring, electronic screens, and artificial skins.[71,131−133] Recently, MXene functionalized flexible strain sensors produced by the electrospinning technique have attracted significant attention owing to their enhanced scalability and ease of fabrication.[134,135] Typically, to fabricate high-performance MXene-based electrospun strain sensors, an elastomer is employed, which acts as the stretchable layer while highly conductive MXenes and other nanofillers are decorated onto the electrospun elastomeric nanofibers. In the current literature, drop-casting,[112] spray coating,[136] electrostatic spraying,[110] and vacuum filtration,[117] are the dominant techniques to deposit MXene nanosheets onto the elastomeric nanofibers to develop MXene-based strain sensors. The elastomeric nanofiber network works as a structural

https://doi.org/10.1021/acsanm.5c02646
ACS Appl. Nano Mater. 2025, 8, 16231−16259

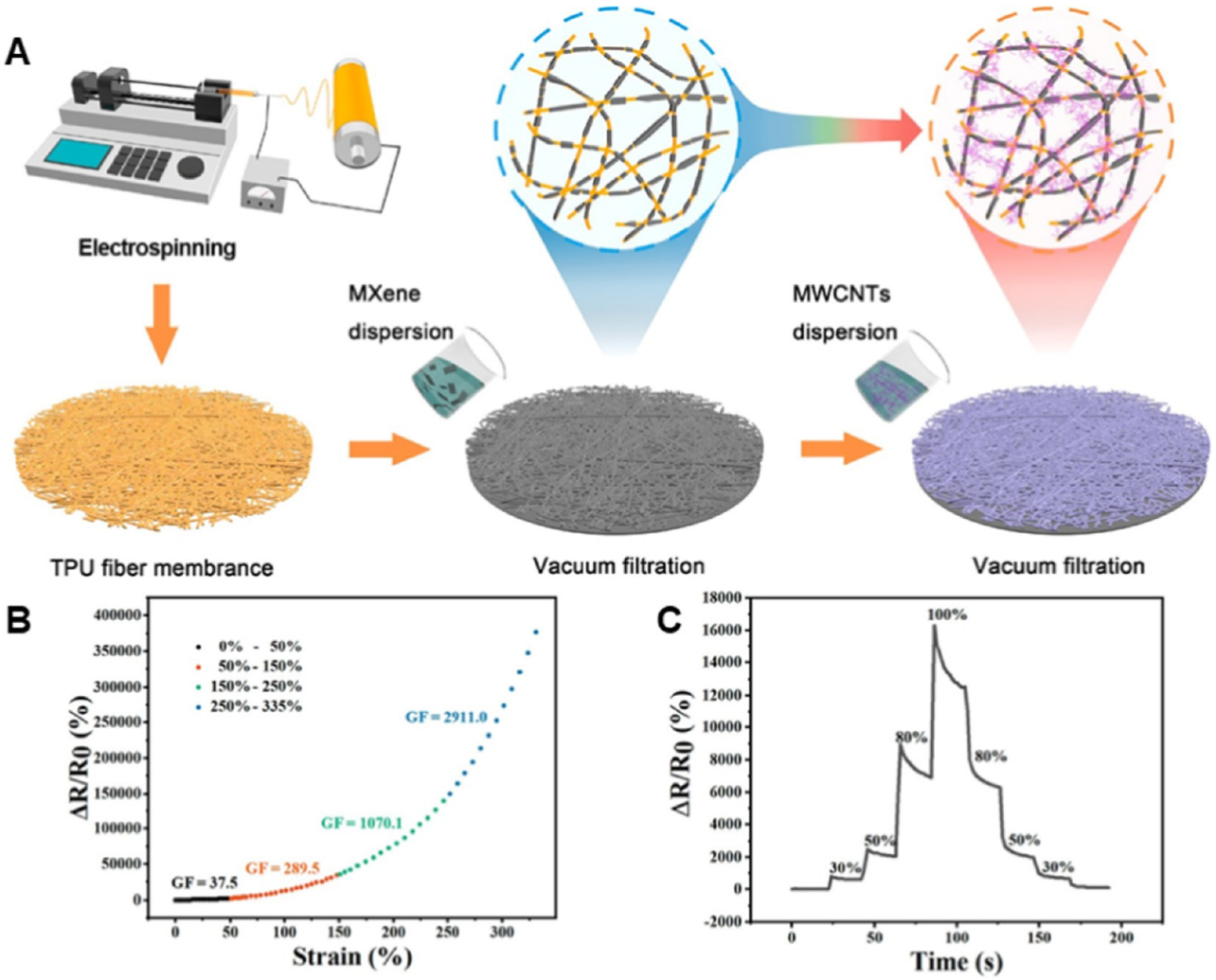

Figure 7. Fabrication and performance of electrospun MXene/CNTs/TPU strain sensors. (A) Protocol for preparing MXene/CNTs/TPU nanofibers. (B,C) Relative resistance of MXene/CNTs/TPU nanofibers as a function of dynamic strain and time. Reprinted with permission from ref 104 Copyright 2022 American Chemical Society.

support for conductive nanofillers (i.e., MXenes) and is able to withstand larger deformations. In recent years, variants of PU,[110] PVDF,[105] and styrene−butadiene styrene (SBS),[117] are some of the common elastomeric polymers utilized repeatedly to fabricate MXene-decorated flexible strain sensors.

While compositing with polymers is a great strategy to combine MXenes into electrospun nanofibers, decorating pre-existing stretchable nanofibers with an MXene coating has been leveraged repeatedly by different research groups. For example, Fang et al.[110] designed a flexible MXene/thermoplastic polyurethane (TPU)-based strain sensor by adopting a unique sandwiched structure. The group first electrospun a TPU layer, followed by the electrostatic spray deposition (ESD) of $Ti_3C_2T_x$ MXene onto the TPU nanofibers. Finally, another TPU encapsulation layer was electrospun onto the MXene sensing layer, rendering a novel sandwiched structured strain sensor. The strain sensor showed stable performance even after 1000 cycles of cyclic loading at 10% strain. Besides, the unique sandwiched structured sensor increased the active strain detecting range by 72%.[110] Li et al.[136] also pursued this strategy and fabricated electrospun MXene/PU strain sensors. The group first electrospun a PU nanofiber membrane, which was further functionalized with MXene nanosheets by a simple spray coating. The as-fabricated strain sensor was highly stretchable and achieved an extremely high gauge factor of 1000 and a wide sensing range up to 270%. This is because the porous network topology of the sensor composite allowed such high sensitivity and wide-range strain detection during dynamic membrane stress.[136]

Levitt et al.[108] developed $Ti_3C_2T_x$ infiltrated-PU nanoyarn strain sensors by a modified bath electrospinning technique. Instead of using a traditional drum collector, an aqueous dispersion of MXene was leveraged as the collector and as a coagulation bath. The as-fabricated yarn strain sensor demonstrated a 60% strain sensing range under repetitive stretching and was highly sensitive up to 20%−50% strain (gauge factor (GF) was ≈17), which could be used for body movement monitoring.[108] In 2022, Dong et al.[104] fabricated a binary structured 2D strain sensor by electrospinning TPU nanofibers and vacuum filtering MXene and carbon nanotube (CNT) solution through the nanofiber membrane (Figure 7A). The TPU skeleton retained mechanical flexibility while the CNT layer and MXene nanosheets synergistically enhanced electrical conductivity. The 2D strain sensor demonstrated an outstanding GF of almost 2911 and an operating strain range of up to 330% (Figure 7B−C). Besides, the sensor demonstrated

https://doi.org/10.1021/acsanm.5c02646
ACS Appl. Nano Mater. 2025, 8, 16231−16259

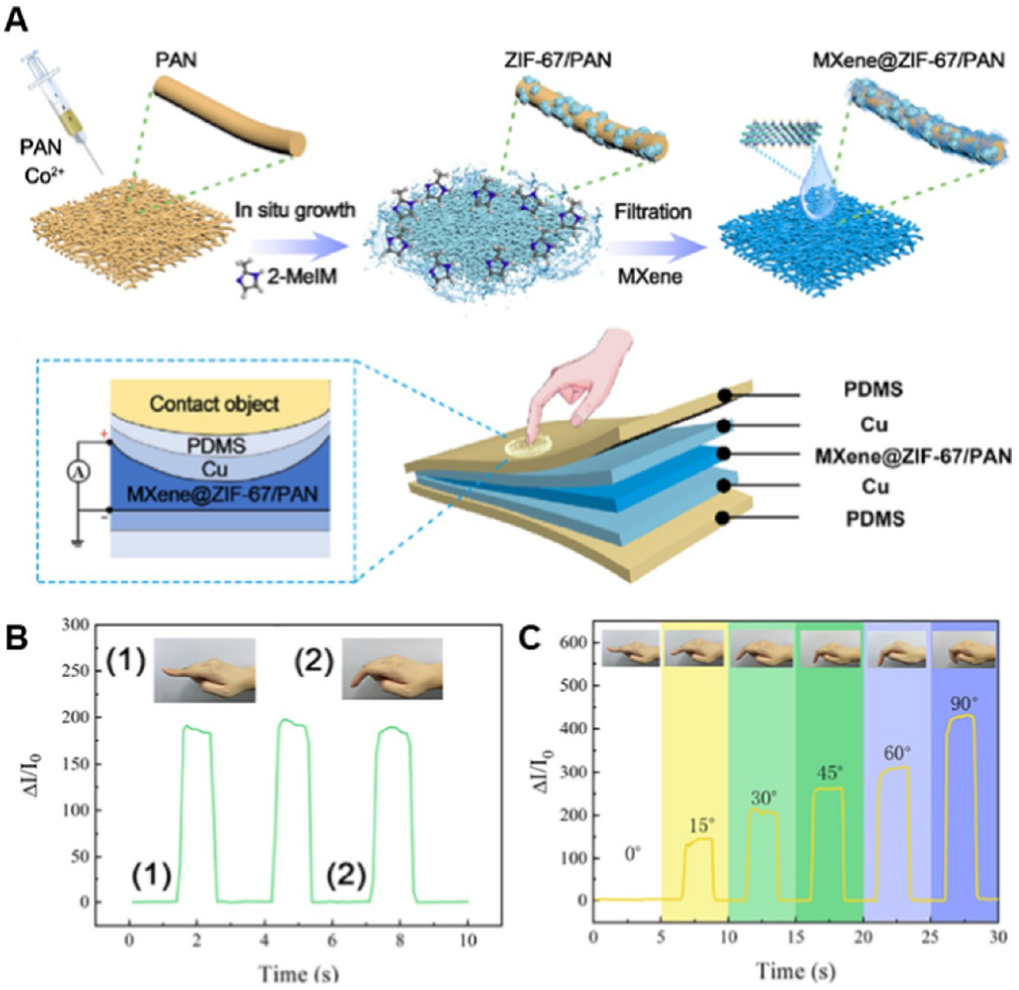

Figure 8. Fabrication and performance parameters of MXene/ZIF-67-PAN nanofiber-based pressure sensors. (A) Scheme depicting the preparation of MXene/ZIF-67-PAN nanofibers. (B,C) Sensor sensitivity in response to dynamic finger deformations. Reprinted with permission from ref 107 Copyright 2022 American Chemical Society.

excellent stability even after 2600 cycles of cyclic strain (50% strain).[104] Using cellulosic materials in composites can act as a building block for sensing applications.[137,138] For example, Taromsari et al.[117] assembled an SBS-based multimodal strain sensor by decorating the SBS nanofiber surface with MXene/graphene nanoplatelets (GnPs)/cellulose nanocrystals (CNCs) following a combined strategy of vacuum filtration and ultrasonic-assisted atomization. The combination of GnPs and MXene demonstrated a synergistic relationship between the two, resulting in high GF (400 at 100% and 76.1 at 10% strain, respectively) and high sensitivity even at lower strain ranges (low detection limit of 0.25% and a short response time of 10 ms). Besides, the addition of CNCs to this composite improved the hydrogen bonding and regularity between MXene and GnPs, enabling the sensor to withstand more than 2000 bending cycles at 100% strain. Such a sensor also demonstrated outstanding performance in monitoring various physiological signals.[117]

5.2. Pressure Sensors. With the ever-increasing demand for portable and wearable electronics, pressure sensors have found numerous applications from electronic skins to continuous healthcare monitoring. Electrospun MXene composite pressure sensors respond to any physical deformation through changing resistance owing to their high conductivity and the transition metal backbone.[56,139] Increasing the MXene loading significantly improves the pressure sensitivity.[56] Many works have been reported on various types of electrospun MXene-based flexible piezoresistive pressure sensors. For instance, piezoresistive pressure sensors operate poorly when there is insufficient dispersion or polarization in the electrospun composite. To address this issue, Liu et al.[61] fabricated flexible $BaTiO_3$/MXene/poly(vinylidene fluoride-trifluoroethylene) (PVDF-TrFE) nanocomposites by electrospinning, where MXene nanosheets enhanced $BaTiO_3$ dispersion, leading to improved polarization and elevating the piezoelectric performance. The as-fabricated pressure sensor delivered a wide detecting range (0.2−400 kPa), quick response (56 ms), and enhanced sensitivity. Besides, the sensor's piezoelectric performance remained stable for up to 5000 compression cycles. Such a sensor exhibited a high prospect as an e-skin for human motion monitoring. Engineering the microstructure of nanofiber webs is an ingenious technique to realize high-performance flexible pressure sensors. For instance, Bi et al.[140] fabricated highly oriented PU/PAN nanofiber webs (OETPN) by increasing the collector rpm to 2800. The as-fabricated OETPN was further spray-coated with MXene nanosheets to act as the active layer. The MXene-coated OETPN was assembled with interdigital electrodes functionalized with silver nanowires (AgNWs) to obtain the final pressure sensor. The as-fabricated pressure sensor demonstrated a high sensitivity of 6.71 kPa^{-1} and was able to operate at a wide sensing range of up to 700 kPa. Such

https://doi.org/10.1021/acsanm.5c02646
ACS Appl. Nano Mater. 2025, 8, 16231−16259

performance could be attributed to the highly oriented microstructure of OETPN, which effectively enhances the overall sensitivity of the pressure sensor. The flexible sensor was also able to monitor radial artery, carotid artery, and speech, showing prospects in healthcare monitoring.[140]

Continuous point-of-care systems heavily rely on wireless biomonitoring of human physiological signals and spatial pressure distributions with negligible environmental impacts. One ingenious strategy is to develop a pressure sensor with degradability and breathability. Chao et al.[111] pursued this approach and fabricated a silk fibroin (SF)-based biodegradable and breathable pressure sensor by electrospinning SF nanofiber membrane, which was further functionalized with MXene by dip coating. The MXene/protein composite pressure sensor achieved a high sensitivity of 298.4 kPa^{-1}, a wide sensing range (up to 39.3 kPa) and a quick response/recovery time. Besides, the pressure sensor showed stable performance after 10,000 cycles of loading−unloading at 70% strain.[111] Fu et al.[107] designed an ultrasensitive pressure sensor using a PAN nanofiber membrane. After electrospinning of PAN nanofibers, ZIF-67 and MXene nanosheets were decorated onto the nanofiber surface via an in situ embedment and drop coating technique (Figure 8A). The assembled highly flexible pressure sensor showed high sensitivity (62.8 kPa^{-1}), wide sensing range (0−100 kPa), and excellent stability (over 10,000 cycles of loading−unloading). The polydimethyl siloxane (PDMS) and copper electrode-supported flexible pressure sensor was implemented for the detection of human body motion, including elbow bending, finger motions, and wrist pulses (Figure 8B,C).[107] Aside from robust support, PDMS was also utilized in fabricating nature-inspired microstructure engraving for pressure sensor applications. For instance, Yan et al.[108] leveraged ginkgo leaf as a template to engrave a unique bionic microstructure on PDMS films, which was functionalized by MXene nanosheets with a facile spray coating. Then, the PVA nanofibrous membrane with an interdigital architecture was electrospun, and the MXene functionalized PDMS film was assembled onto the membrane to achieve the final pressure sensor. The ginkgo leaf-inspired protuberances were highly squishy, and with the increase in pressure, the contact area increases, which in turn enhances the overall sensitivity of the pressure sensors. The assembled pressure sensor demonstrated a wide operating range (0−18 kPa), an ultrahigh sensitivity of 403.46 kPa^{-1}, a fast reaction time of 99.3 ms, and remarkable durability with 12,000 pressure cycles. The pressure sensor showed high prospects in human physiological signal detection and also in human−computer interactions.[106]

5.3. Gas Sensors. Identification and measurement of gaseous species, such as (CO, NO, CO_2, NO_2, NH_3, H_2S, NH_3, H_2, CH_4, N_2, and O_2) and VOCs are crucial for monitoring air quality, emissions, and for ensuring industry safety.[141−143] Electrospun MXene thin nanocomposites are highly favored for gas sensing applications because of their active zones, conductivity, variable surface chemistry, and exceptional durability.[90,141,144,145] Compared to drop casting, vacuum filtration, and dip coating, MXene nanocomposite films produced by the electrospinning are thinner, resulting in a superior surface area with enhanced gas-detecting capabilities.[78,146]

MXene coating onto electrospun flexible nanofiber membranes works as an efficient gas-sensing element to detect NH_3. For instance, Sardana and Mahajan[147] prepared a cellulose nanofibrous membrane by electrospinning cellulose acetate (CA) polymer. The MXene aqueous solution was then drop-cast onto the cellulose nanofiber (CNF) membrane to achieve the final MXene/CNF gas sensor composites. The as-fabricated sensor exhibited a high selectivity toward NH_3, excellent sensing response even at an ultralow concentration of 5 ppm, and a faster response−recovery rate of 42/69 s.[147] Apart from coated gas sensors, MXene-based self-powered gas sensors were also reported. For instance, in a 2022 study, Sardana et al.[116] leveraged electrospun MXene/PVA nanofibers (electronegative layer) and CA nanofibers (triboelectric layer) to act as triboelectric nanogenerators, which could seamlessly power MXene/TiO_2/C-NFs heterojunction-based gas sensor to detect NH_3 with excellent sensitivity (1−100 ppm). MXene/TiO_2/C-NFs composites were assembled utilizing a facile vacuum filtration technique. The MXene-based TENG provided a power density of ∼1361 mW/m^2 at 2 MΩ. Besides, the chemiresistive sensor showed a high selectivity toward NH_3, outstanding reproducibility, and an enhanced response/recovery time (76 s/62 s) at ambient temperatures.[116]

In recent years, electrospun transition metal oxide fibers (TMOs) have gained considerable popularity in fabricating MXene-based gas-sensing nanocomposites. In order to electrospin TMOs, polyvinylpyrrolidone (PVP) is repeatedly combined with numerous TMOs to achieve the desired TMO nanofibers. The as PVP-assisted TMO nanofibers were then subjected to hydrothermal or electrostatic self-assembly to fabricate the gas-sensing composites. For instance, Ma et al.[148] leveraged the electrospinning technique to prepare ammonium heptamolybdate ($(NH_4)_6Mo_7O_{24}$)/polyvinylpyrrolidone (PVP) nanofibers, which were subsequently calcinated and mixed with aqueous MXene solution. The composite solution was used as an ink that was coated onto an electrode system using an l-*b*-l approach to detect highly toxic trimethylamine (TMA) gas. The nanocomposite sensor showed excellent selectivity, ultralow detection limit, and fast response rate (10 s/7 s).[148] Similarly, Xie et al.[149] first electrospun In_2O_3/PVP nanofibers and prepared In_2O_3/MXene composites by an electrostatic self-assembly technique. The In_2O_3/MXene composite gas sensors showed a stable response at lower concentrations (50 ppm of TMA), achieved a fast response/recovery rate (4/3 s), low functioning temperature (120 °C), and excellent selectivity.[149] Leveraging a similar approach, in early 2024, Sun et al.[150] and in later months the same group,[151] in 2023 Gasso and Mahajan[152] reported $ZnSnO_3$/ZnO/$Ti_3C_2T_x$ MXene, $LaFeO_3$/$Ti_3C_2T_x$ MXene, and SnO_2/MXene gas sensors to detect acetone, formaldehyde, and NO_2, respectively.

MXene-based gas sensors are also investigated to detect VOCs. VOCs must be recognized since they contribute to air pollution. For instance, Yuan et al.[112] first electrospun a hybrid nanofiber membrane with a 3D porous architecture consisting of PVA and polyetherimide (PEI) onto a flexible interdigital Au electrode. The PVA/PEI assembly was further modified with MXene nanosheets by a simple drop-casting technique to achieve the final gas-sensing element. The as-fabricated gas sensor was highly selective toward various VOCs (acetone, methanol, ethanol) at the ppb level. The gas sensor also offered enhanced sensitivity (0.10−0.17 ppm^{-1}), a fast response-recovery rate (less than 2 min), and a wide sensing range (ppb to saturated vapor). The VOC sensor proved incredibly resilient (no degradation for 1000 bending cycles). Such high performance is highly conducive to detecting and remedying VOCs in the atmosphere.[112] Apart from coated gas sensors, polymer

https://doi.org/10.1021/acsanm.5c02646
ACS Appl. Nano Mater. 2025, 8, 16231−16259

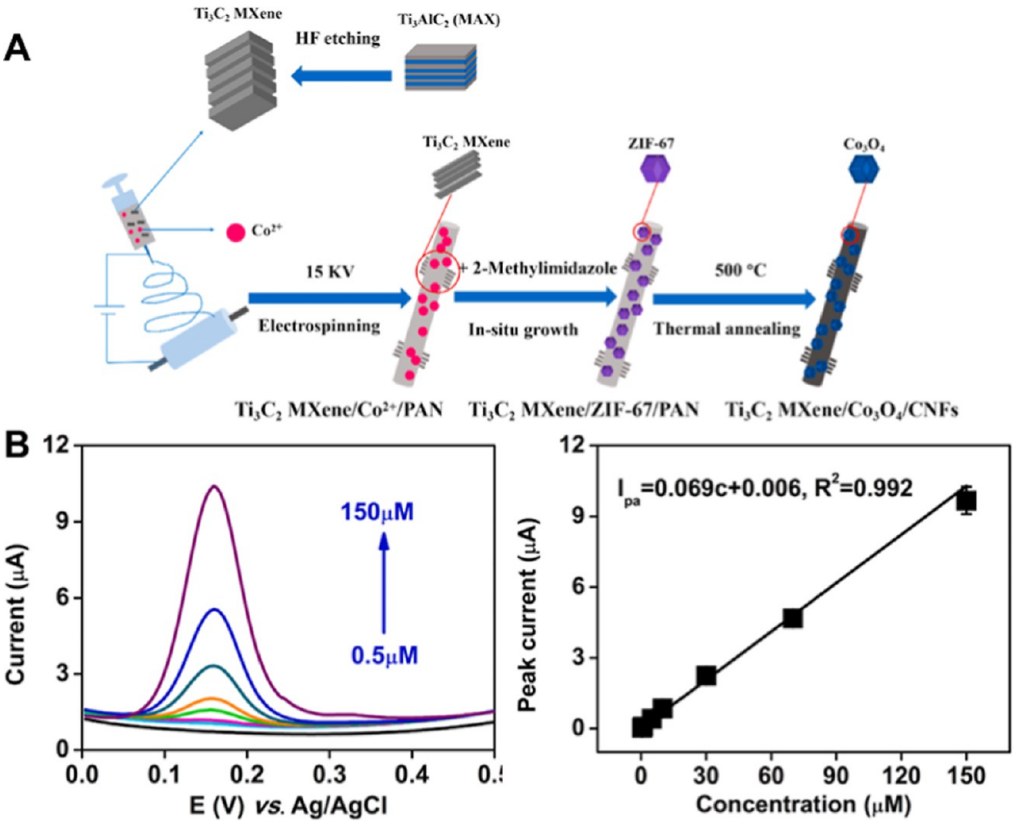

Figure 9. VOC detection with flexible MXene-based electrospun sensors. (A) Protocol for fabricating electrospun Ti_3C_2 MXene/Co_3O_4/CNFs gas sensors. (B) 4-AP detection performance at varying concentrations and its corresponding calibration curve. Reprinted with permission from ref 71 Copyright 2023 Elsevier Ltd.

composite gas sensors have also been reported in recent years. For instance, Cheng et al.[71] fabricated a PAN/Co^{2+}/Ti_3C_2 MXene composite nanofibers by an electrospinning technique. The divalent Co ion acted as a template to grow ZIF-67 following a hydrothermal reaction, which was thermally annealed into Co_3O_4 to further increase the surface area (Figure 9). The obtained Ti_3C_2 MXene/Co_3O_4/CNFs nanocomposite demonstrated enhanced 4-aminophenol (4-AP) sensitivity, was highly selective, offered a wide sensing range (0.5 to 150 μM), and an ultralow detection limit of 0.018 μM was reported.[71]

The performance of VOC sensors is influenced by several critical variables. Sensitivity determines the sensor's ability to detect low concentrations of VOCs, while selectivity ensures accurate identification of specific VOCs in the presence of interfering gases. Response time and recovery time reflect how quickly the sensor reacts to VOC exposure and returns to its baseline state. The limit of detection defines the minimum detectable concentration. Operating temperature affects adsorption and desorption behavior, impacting sensor accuracy. Humidity tolerance is important, as moisture can interfere with sensor output. Stability and repeatability represent the sensor's long-term consistency and performance over multiple cycles. The surface area and porosity of the sensing layer enhance VOC adsorption. Finally, electrical conductivity or capacitance governs signal transduction. These parameters collectively determine the sensitivity, reliability, and applicability of VOC sensors for real-world environmental or biomedical monitoring.[124,153−155]

5.4. Self-Powered Sensors. In order to power microelectronic devices by generating electricity from the surrounding environment, a variety of energy harvesting methods, including piezoelectric, electromagnetic, and triboelectric, have recently been investigated. Based on these phenomena, triboelectric nanogenerators (TENGs) and piezoelectric nanogenerators (PENGs) coupled with an MXene-based sensing system are becoming increasingly popular in self-powered electronic devices owing to their lightweight nature, high-power density, and accessibility.[156−159] While there remain many strategies to fabricate self-powered sensors, MXene-integrated electrospun sensors with an energy harvesting unit have been gaining considerable attention in the past few years (2021−2024). This is because improved power production efficiency is ensured owing to electrospun nanofibers large surface area and pores.[160]

By electrospinning a high-performance flexible poly(vinyl alcohol) (PVA)/MXene composite nanofibers film, Wang et al.[57] fabricated a self-powered humidity sensor. These composite nanofibers were later inserted onto flexible polyethylene terephthalate (PET)-supported $MoSe_2$ PENG, which was able to produce a peak output of 35 mV and a power density of 42 mW/m^2 scavenging energy from different parts of the human body. Such a self-powered MXene-based sensor achieved a fast response-recovery time (0.9/6.3 s), a low hysteresis (1.8%), and outstanding repeatability.[57] Abreast of $Ti_3C_2T_x$ MXene, other MXene variants are implemented to fabricate self-powered flexible sensors. For instance, Faruk et al.[81] fabricated a novel V_2CT_x MXene-based self-powered pressure sensor for simultaneous biomechanical energy harvesting and real-time human activity monitoring. The electrospun V_2CT_x/poly(vinylidene-fluoride-*co*-hexafluoropropylene) (PVDF-HFP) (VPCN) nanofibers worked as an electronegative layer owing

https://doi.org/10.1021/acsanm.5c02646
ACS Appl. Nano Mater. 2025, 8, 16231−16259

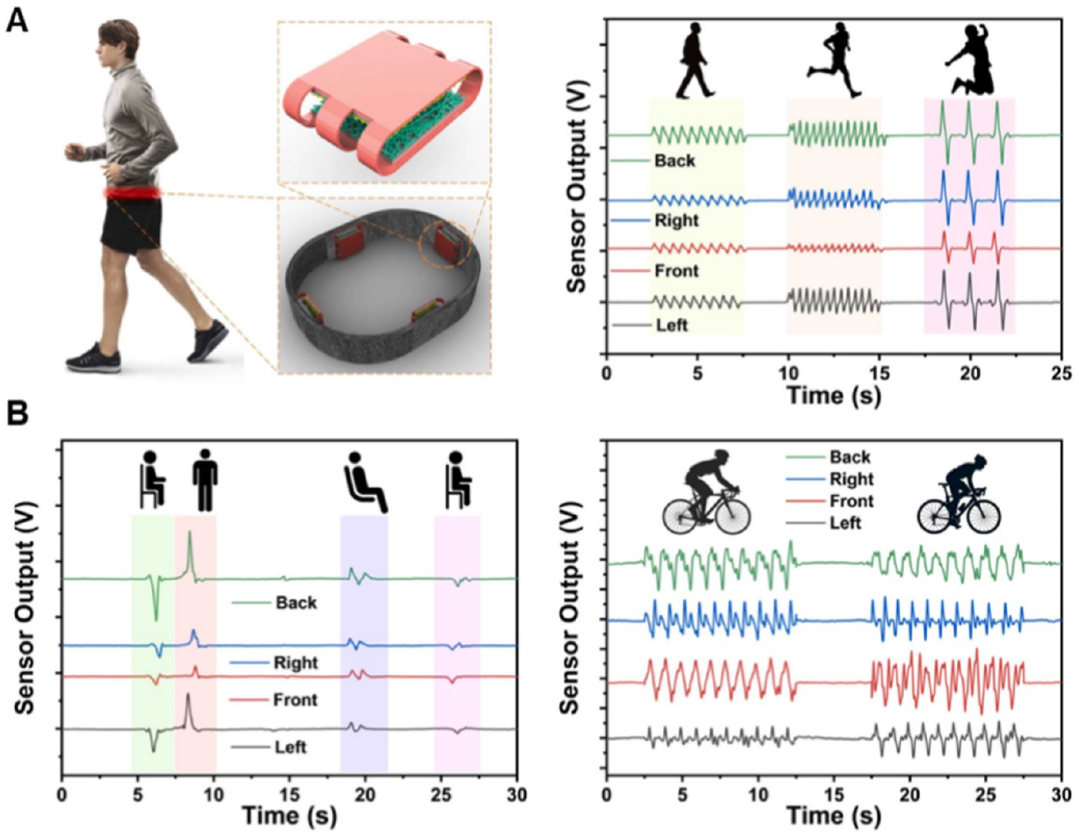

Figure 10. (A) VPCN-TENG-supported wearable belt worn by a human being and its corresponding sensor responses toward various human activities (walking, running, and jumping). (B) Human posture monitoring with VPCN-TENG-supported wearable belt during sitting and cycling. Reprinted with permission from ref 81 Copyright 2024 Elsevier Ltd.

to MXene's abundant surface terminations. In addition, integrating V_2CT_x within the PVDF-HFP nanofiber architecture improved the charge trapping capability as well as enhanced the dielectric constant. When combined with electrospun PEO nanofibers, the VPCN-TENG delivered a peak power density of 18.20 W/m^2. The assembled VPCN-TENG was further investigated as a self-powered pressure sensor to monitor human activity, which achieved a high sensitivity of 25.17 V/kPa (1−42 kPa) (Figure 10).[81]

PVDF and its copolymers are dominant in fabricating MXene-based TENG/PENG-driven self-powered sensors. For example, Pan et al.[161] leveraged near-field electrospinning to implement AgNPs and $Ti_3C_2T_x$ MXene into PVDF nanofiber architecture. The assembled nanocomposite exhibited outstanding piezoelectric performance when an external force was applied (peak voltage 5−15 V). The light-emitting diode (LED) demonstrations revealed the potential of PVDF/AgNP/MXene nanofibers in simultaneous energy harvesting and powering microelectronic systems.[161] In another work, Rana et al.[162] fabricated PVDF-TrFE/MXene nanocomposite fibers to detect human motions. The as-fabricated PVDF-TrFE/MXene nanofibers worked as an electronegative tribolayer since the implementation of 10 wt % MXene into PVDF resulted in enhanced surface charge density and dielectric constant. Coupled with an electropositive nylon-11 nanofibrous mat, the assembled self-powered sensor achieved a power density of 4.02 W/m^2 at 6 Hz, an enhanced sensitivity of 1 V/kPa, and excellent repeatability (up to >20,000 cycles). The fabricated self-powered sensor was able to control home appliances by just detecting human motion.[162] Apart from PVDF and its copolymers, other functional polymers are also utilized for fabricating MXene-based self-powered sensors. For instance, Wang et al.[163] developed a CNT/MXene-based self-powered pressure sensor coupled with solar cells and microsupercapacitor (MCS) unit, all integrated onto an electrospun poly(styrene−ethylene/butylene−styrene) (SEBS) flexible film. After electrospinning of CNTs-SEBS film, the MXene aqueous solution was vacuum filtered to achieve the CNTs/SEBS-MXene nanocomposites for self-powered pressure sensing. The as-fabricated sensor showed a GF ranging from 286 to 36,406, a fast response-recovery time (87.60 ms/87.62 ms), and an excellent cyclic stability after 10,000 cycles of bending/release. The high sensitivity of the sensor allowed capturing the facial microexpressions of humans and word detection.[163]

5.5. Electrochemical Sensors. Electrospun 2D MXene composites have good electrical conductivity, novel surface chemistry, and mechanical robustness, making them suitable for electrochemical sensing applications.[164] The electrochemical sensors are utilized for detecting different organic and inorganic chemical compounds in various sectors such as pharmaceuticals, biomedical, clinical, and food industries. Despite such potential, the reports on MXene-based electrochemical sensors fabricated via an electrospinning technique remain scarce. In recent years, however, research on MXene-functionalized electrochemical sensors fabricated by electrospinning has been advancing and gaining considerable attention. MXene-based electrospun electrochemical sensors have now been widely implemented to detect numerous bioanalytes, drugs, and persistent environmental pollutants.[58,165]

https://doi.org/10.1021/acsanm.5c02646
ACS Appl. Nano Mater. 2025, 8, 16231−16259

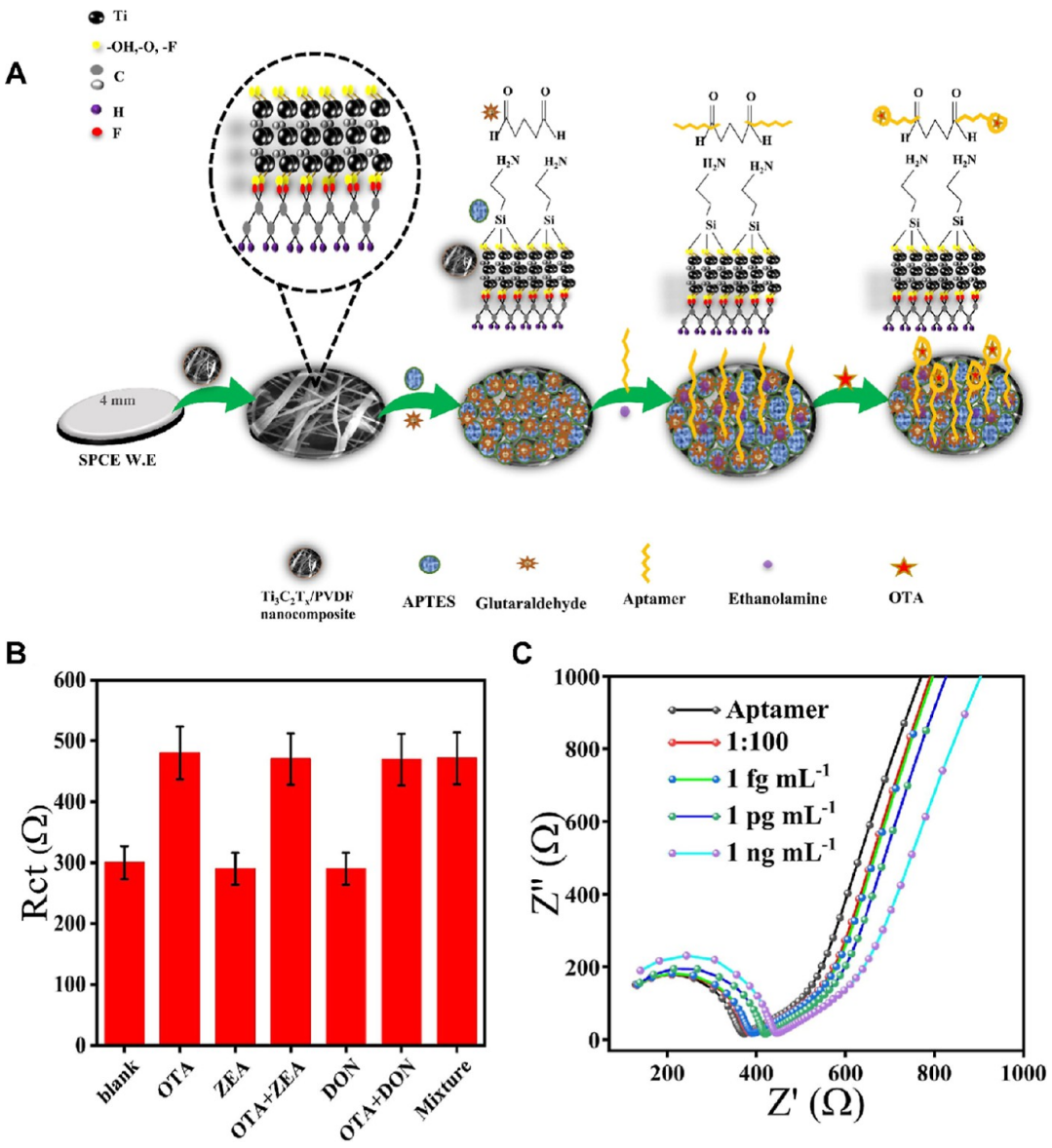

Figure 11. MXene-based electrochemical sensors for detecting OTA. (A) Schamatic illustration depicting the fabrication and sensing mechanism of APTES functionalized MXene/PVDF aptasensors. (B) Selectivity toward OTA, (C) Analytical performance of APTES-modified $Ti_3C_2T_x$/PVDF sensors to detect OTA. Reprinted with permission from ref 58 Copyright 2022 Elsevier Ltd.

Combining electrospun TMO fibers with MXene remains an effective strategy for fabricating TMO-functionalized MXene nanocomposite electrochemical sensors. For instance, leveraging the unique one-dimensional (1D) architecture of TMO nanofibers and 2D MXene nanosheets, Ranjith et al.[166] prepared MXene-$FeWO_4$ nanohybrid for the detection of Rutin (3′,4′,5,7-tetrahydroxy-flavone-3-*d*-rutinoside) (RTD). The group first electrospun $FeWO_4$ nanofibers by mixing TMO precursors with PAN and poly(methyl methacrylate) (PMMA) at a ratio of 60/40. The electrospun $FeWO_4$ nanofibers were further combined with $Ti_3C_2T_x$ nanosheets following a hydrothermal route to assemble the final MXene-$FeWO_4$ nanocomposite electrochemical sensors with a 2D-1D architecture. The as-prepared nanocomposite sensor achieved an outstanding linearity (4−147 nM) at an ultralow limit of detection (LOD) of 0.42 nM and an enhanced sensitivity of 0.3799 μA/nM cm^2 for detecting RTD electrochemically. The catalytic characteristics of the composite were enhanced when promoter flaws were present in its micro/nanostructure. This showed remarkable precision in the RTD detection of human blood. In a later study, the same group adopted the previous approach by combining $MnMoO_4$ with MXenes.[167] The group fabricated $MnMoO_4$ nanofibers by mixing PAN and PMMA with transition metal precursors. The $MnMoO_4$ nanofibers and MXene nanosheets were further fabricated into $MnMoO_4$−MXene nanocomposites by a simple hydrothermal method. The unique interface produced by 1D $MnMoO_4$ nanofibers and 2D MXene nanosheets within the nanocomposite delivered a broad sensing range (5−65 nM) and an ultralow detection limit for hydroquinone (0.26 nM) and catechol (0.30 nM). The assembled electrochemical sensor was highly conducive to detecting hazardous pollutants in industrial wastewater.[167]

Apart from traditional electrochemical sensors, MXene-based electrospun sensors are finding applications as aptasensors to detect dangerous toxins. For instance, Al-Dhahebi et al.[58] developed an ultrasensitive electrochemical aptasensor based on PVDF/MXene electrospun nanofiber membrane to detect Ochratoxin A (OTA). The nanocomposites were further

https://doi.org/10.1021/acsanm.5c02646
ACS Appl. Nano Mater. 2025, 8, 16231−16259

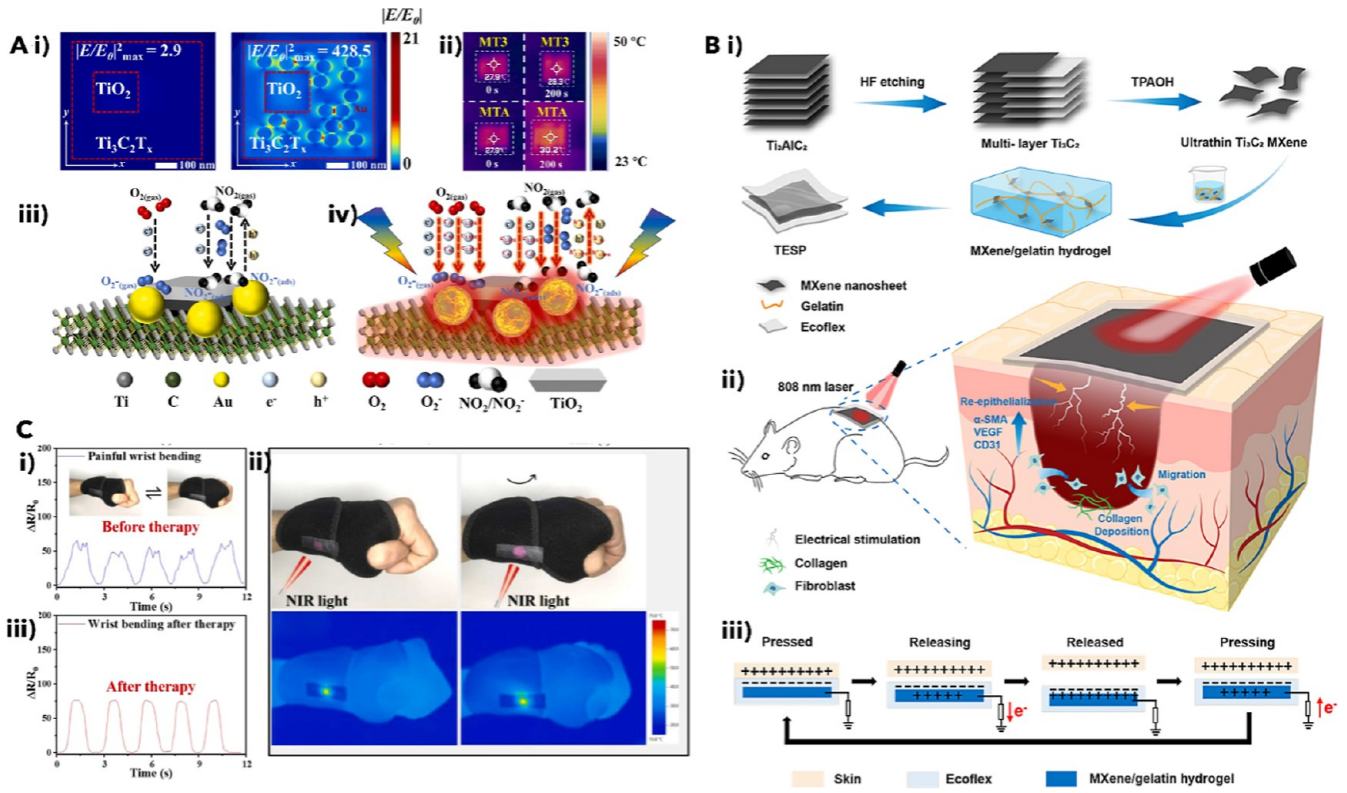

Figure 12. (A) (i) Normalized electromagnetic field distribution on MT3 and MTA samples. (ii) Infrared thermal images of MT3 and MTA sensors before and after 530 nm light irradiation (200 s intervals). Schematic illustration of NO_2 sensing mechanism (iii) without and (iv) with 530 nm light exposure. Reprinted with permission from ref 171 Copyright 2024 Elsevier B.V. (B) Schematic of MXene-based TENG electronic skin patch (TESP): (i) fabrication using MXene/gelatin hydrogel, (ii) NIR-assisted wound healing, and (iii) working mechanism of wearable TESP. Reprinted with permission from ref 172 Copyright 2024 Elsevier B.V. (C) MXene-based photothermal-therapy epidermic sensor (i) Sensing performance of the wearable sensor on a volunteer's wrist before photothermal therapy, (ii) Wrist bending under 808 nm NIR irradiation with corresponding IR thermal images, and (iii) Sensing performance after photothermal heating and therapy. Reprinted with permission from ref 173 Copyright 2023 Elsevier Ltd.

functionalized with (3-Aminopropyl) triethoxysilane (APTES), and OTA aptamer was immobilized onto the nanocomposite surface (Figure 11A). The synergistic combination of PVDF and MXene nanosheets was proficient in acting as an electrochemical redox probe, which enhanced the aptamer-OTA interactions. The as-prepared MXene-based electrochemical sensor achieved high selectivity and an enhanced sensitivity of LOD of 2.15 fg/mL and a limit of quantification (LOQ) of 6.52 fg/mL while maintaining a wide linear detection range from 1 fg/mL to 1 ng/mL (Figure 11B,C). Such a high selectivity and sensitivity of such sensors opens up a potential platform for detecting OTA in food and beverages.[58]

In addition to the electrochemical detection of bioanalytes, MXene-based electrospun electrochemical sensors are also leveraged for environmental monitoring applications. For example, Taromsari et al.[168] leveraged coaxial electrospinning to fabricate SBS/cetrimonium bromide (CTAB) nanofibers for electrochemical NH_3 gas detection. The SBS/CTAB nanofibers were further coated with graphene nanoribbons (GnR) and MXene to achieve the final 3D-structured electrochemical sensing unit. The hybridization of GnR with MXene elevated the bandgap from 2.72 to 3.51 eV, which enhanced the NH_3 gas sensing capabilities. In addition, the sensor achieved a wide sensing range (40 ppb−6000 ppm) owing to the high specific surface area of the nanocomposites. The presence of GnR/MXene active sites imparted sensitivity under bending with strong environmental stability, making the sensor appropriate for wearable applications.[168]

5.6. Photothermal Sensors. Photothermal sensing is a technique in which materials convert absorbed light—typically in the near-infrared (NIR) region, into localized heat, enabling temperature detection through the resulting thermal response. MXenes, especially $Ti_3C_2T_x$, are highly effective photothermal agents due to their strong broadband optical absorption, high thermal conductivity, and efficient light-to-heat conversion. When incorporated into flexible substrates or polymer matrices, MXenes enable precise light-triggered thermal sensing. For instance, under NIR irradiation, the photothermal effect causes a rapid and localized increase in temperature, which can be monitored using thermoresistive elements or infrared detectors. This property allows for remote, noncontact temperature sensing with fast response times, making MXene-based photothermal sensors suitable for wearable health monitoring, thermal mapping, and on-skin diagnostics. Zong et al.[169] developed a multifunctional hydrogel sensor by combining MXene-coated silk nanofibers with poly(vinyl alcohol), leading to a uniform conductive network. It showed high tensile strength (5.07 MPa), large strain range (700.6%), high sensitivity (gauge factor 8.2), and electrical conductivity (1.64 S/m). It enabled physiological sensing, speech recognition, and photothermal heating to 82.8 °C. Tang et al.[170] developed a conductive Janus nanofiber composite by layering MXene/chitosan and MXene/polyurethane nanofibers to create asymmetric wettability. It showed rapid unidirectional water transport (10 s) and antigravity water movement (18 s). The material demonstrated excellent durability, photothermal response, temperature

https://doi.org/10.1021/acsanm.5c02646
ACS Appl. Nano Mater. 2025, 8, 16231−16259

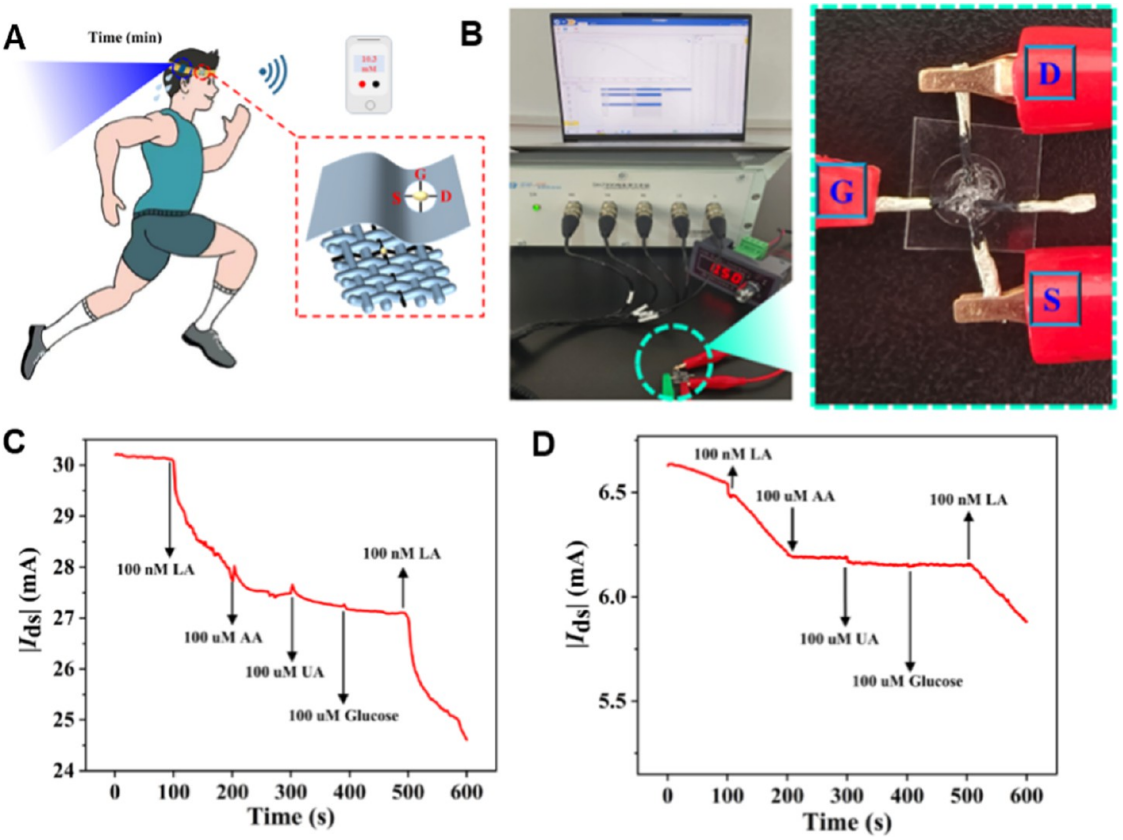

Figure 13. Electrospun MXene nanocomposite fabric toward real-time lactate detection from human sweat. (A) Scheme depicting the real-time monitoring of lactate while running. (B) Lactate detection test set up. (C,D) Cyclic performance of MXene-based lactate sensors. Reprinted with permission from ref 181 Copyright 2023 Elsevier B.V.

sensing, and flexibility, making it ideal for smart wearable electronics.

A plasmonic photothermal strategy was developed by Hu et al.[171] to overcome the poor sensitivity and sluggish response of MXene-based gas sensors at room temperature. A $Ti_3C_2T_x$/TiO_2/Au (MTA) heterostructure was synthesized, where Au nanoparticles enhance light absorption and localized heating via the localized surface plasmon resonance (LSPR) effect. Under 530 nm light irradiation, the MTA sensor demonstrated a significantly improved response to 1 ppm of NO_2—7.6× and 2.34× higher than $Ti_3C_2T_x$/TiO_2 and MTA in dark, respectively. Infrared imaging confirmed a localized temperature rise due to photothermal conversion. Finite-Difference Time-Domain simulations revealed strong electric field enhancement near Au nanoparticles (NPs), facilitating photocarrier generation and accelerating gas-sensing reactions. The combined effects of hot electron injections, increased adsorption/desorption kinetics, and localized lowering of the activation energy improve sensitivity, selectivity, and response/recovery times (Figure 12A). Mao et al.[172] developed a self-powered photothermal triboelectric skin patch (TESP) based on MXene/gelatin hydrogel to enhance wound healing. The MXene provided excellent conductivity and photothermal conversion, while gelatin offered flexibility and phase-transition capability. At 10% MXene content, the TESP generated peak outputs of 163.7 V and 8.1 μA under 60 N force at 2 Hz and retained performance after 6000 cycles. Upon 808 nm NIR irradiation, TESP reached 58.3 °C in 500 s, accelerating cell migration in vitro and boosting re-epithelialization and collagen formation in vivo. On Day 5, the TESP + NIR group showed a re-epithelialization rate of 76.2%, outperforming all controls. On Day 10, collagen deposition increased to 60.3%. Additionally, the TESP served as a motion sensor, producing a 5.8 V signal upon finger contact (Figure 12B).

Electronic sensor developed by Chao et al.[173] using a MXene/AgNW-based nanofiber network demonstrated excellent photothermal properties for integrated health monitoring and therapy. Upon exposure to 808 nm near-infrared (NIR) light, the sensor exhibited efficient photothermal conversion, enabling localized heating suitable for on-demand therapy. The temperature rise was tunable by adjusting light power density (0.25−1.5 W/cm^2) and monitored using infrared thermal imaging (Figure 12C). This photothermal effect enhances antibacterial performance and accelerates wound healing by promoting blood flow and tissue regeneration. Additionally, the sensor simultaneously enables strain sensing, making it ideal for dual-mode functionality—thermal treatment and physiological signal detection. The ability to combine light-triggered heating with electrical sensing in a soft, wearable form factor provides a powerful tool for real-time diagnostics, therapy, and recovery tracking. Moreover, tunable surface terminations can further enhance interfacial heat transfer and compatibility with polymers. Challenges in this sensing system include maintaining long-term photothermal stability and minimizing signal drift during repeated irradiation cycles.

5.7. Biosensors. Owing to MXene's surface termination, electrical conductivity, and enhanced biocompatibility, this unique 2D material has found numerous applications in wearable biosensing and bioelectronics.[174,175] Numerous variants of MXene have been demonstrated to be nontoxic to

https://doi.org/10.1021/acsanm.5c02646
ACS Appl. Nano Mater. 2025, 8, 16231−16259

living organisms. Early transition metals such as tantalum (Ta), niobium (Nb), and titanium (Ti) have shown relatively inert behavior toward living cells. Recent studies have also confirmed that MXenes can degrade within the living body, highlighting their biocompatibility and potential for biomedical applications.[176−178] Owing to their exceptional properties, MXenes have found applications in a wide range of biological fields. They are being used in biosensing, bioimaging, disease diagnosis, and therapeutics. Additionally, MXenes show promise in implants and even as antibacterial agents, making them a versatile tool in healthcare and medicine.[179−181] In this context, MXene-based biosensors fabricated by the electrospinning technique have been gaining considerable popularity among other sensing platforms.

MXene-based electrospun composites have been employed in wound management and real-time biochemical sensing applications. For instance, Zizhou et al.[182] fabricated an artificial vascular graft by leveraging 2D MXene (Ti_3C_2) nanosheets embedded in PMMA/PDMS nanofiber composites. The group reported that the resultant composites showed less cytotoxicity at 20 wt % of MXene. Besides, the graft was stable even after being exposed to physiological environments.[182] In another study, Shen et al.[181] leveraged electrospinning to fabricate polyvinyl formal (PVF)-based sweat sensing interface functionalized with MXene nanosheets and conductive poly(3,4-ethylenedioxythiophene) polystyrene sulfonate (PEDOT:PSS). The PVF/MXene/PEDOT:PSS and PVF/PEDOT:PSS nanofibers were further assembled into fiber-based organic electrochemical transistors (FECTs) for real-time lactate detection from human sweat (Figure 13A). The PVF/MXene/PEDOT:PSS-based FECT had a good linear correlation with lactate concentration and achieved a high sensitivity of 0.442 NCR/decade. Besides, the fabricated sweat sensor offered a wider sensing range of 1 nM-100 mM, ultrafast response time (5 ms), and outstanding reproducibility (Figure 13B−D). Such enhanced performance could be attributed to the high specific surface area of PVF nanofibers, along with the elevated conductivity contributed by MXene and PEDOT:PSS. The incorporation of MXene ensured the stability of PEDOT:PSS to the PVF nanostructures and synergistically increased the sensitivity of the flexible sensor by improving redox kinetics at the interface.[181]

MXene functionalized electrospun composites can be employed as a multiscale sensing platform for detecting a range of physical and chemical biosignals. Sharifuzzaman et al.[121] leveraged an electrospun MXene/fluoropolymer nanofiber-integrated composite electrodes for human sweat glucose monitoring, pH detection, and real-time electrocardiogram (ECG) recording. After electrospinning MXene/fluoropolymer composites, the mat was carbonized using a CO_2 laser, which resulted in a thermal activity-induced inhomogeneous generation of TiO_2 nanoparticles on the 3D structure. The fabricated sweat-sensing soft bioelectrode achieved a sensitivity of 77.12 μA/mm cm^2 within the physiological range of 10 μM to 2 mM. Besides, it also achieved an ultralow detection limit of 10 μM with a linear range of 10 μM to 2 mM, appropriate for detecting glucose from human sweat. Additionally, the electrode showed a pH sensitivity of −55.89 mV/pH within an accurate pH sensing range of 3−9. It can also monitor ECG signals with an SNR of 37.63 dB during static and 21.69 dB for dynamic activity, respectively.[121]

In addition to multifunctional biosensing platforms, interest has been rising in fabricating biodegradable MXene-based electrospun sensing composites. For instance, Huang et al.[183] developed a polylactic acid (PLA)/MXene sensing composite for wearable biomonitoring and investigated its biodegradability. After electrospinning PLA nanofibers, MXene nanosheets (concentration-5−20 mg/mL) were coated onto the PLA mat to achieve the biomonitoring electrode for wrist pulse detection and speech recognition. The fabricated pressure sensor from the composite electrode achieved a high sensitivity of 5.37 kPa^{-1} with a fast response time (98 ms). Besides, the composite sensor was highly durable, achieving 6000 cycles of loading and unloading at 50 kPa with minimum signal deviation (<3.4%). In addition, the MXene/PLA composite showed efficient degradation in 1 wt % sodium carbonate solution (pH = 11.6). Such accelerated degradation can be attributed to the MXene coating, which improved the water absorption and was conducive to bond hydrolysis.[183] Table 3 summarizes the applications of MXene functionalized electrospun composites for flexible sensing applications.

6. SUMMARY, CHALLENGES, AND PERSPECTIVES

We have critically summarized the synthesis and classification of MXenes, flexible sensing mechanisms, electrospinning process factors, and last, the various application fields of MXene-based electrospun nanocomposites for flexible sensing applications. Tremendous progress has been made in the field of MXene-based electrospun flexible and wearable sensors. While there remain many MXene variants, to date, $Ti_3C_2T_x$ remains the most widely adopted MXene for fabricating electrospun flexible sensors. In terms of flexible sensing, the piezoresistive, capacitive, and piezoelectric principles govern the functions of strain and pressure sensors. In contrast, triboelectric and chemiresistive principles govern the functions of self-powered sensors, biosensors, and electroschemical sensors, respectively. As for the electrospinning process, polymer type, MXene loading, solvent used, and electrospinning parameters (voltage, distance, drum speed, etc.) affect the nanostructure (diameter, surface area) of the fabricated MXene-based fibers. Lastly, we critically summarized and reported the state-of-the-art application of such nanofibers in a myriad of flexible sensing applications, such as pressure, strain, gas, self-powered, photothermal, electrochemical, and biosensors.

Although MXene-based electrospun nanocomposites in flexible sensing research are expanding, such composites face some significant drawbacks for real-world applications. For instance, current MXene synthesis (i.e., HF etching) is expensive and detrimental to the environment. Besides, MXenes tend to agglomerate in polymer dispersion and thus reducing conductivity and mechanical reinforcement. In addition, the cost and accessibility of the final MXene-based flexible sensors also impose additional challenges on the sensors design, fabrication, and implementation. Besides, MXenes tend to degrade and oxidize over time in humid and high-temperature environments. Owing to the reactivity of the transition metal (M) layer with oxygen and water molecules, stable metal oxide (i.e., TiO_2) and amorphous carbon form at the edges and defect sites, decreasing the conductivity. As a result, the cyclic stability and reliability of such flexible sensors in these environments are not applicable for long-term applications. Apart from this, the overall sensing performance of MXene-based flexible sensors is not satisfactory. Taking the MXene-based flexible pressure sensor as an example, the sensors have comparatively low response times and narrow detection limits. MXene-based gas sensors, on the other hand, suffer from low selectivity and

https://doi.org/10.1021/acsanm.5c02646
ACS Appl. Nano Mater. 2025, 8, 16231−16259

Table 3. MXene Functionalized Electrospun Sensors for Multifaceted Applications

sensor type	composition	sensing mechanism	sensor performance	response/recovery time	reference
strain sensors	TPU-MXene	resistive	strain range-70%	1000 cycles of loading at 10% strain	110
	PU-MXene	piezoresistive	GF-1000, Ultra low detection limit, 0.05% for tensile strain, a wide sensing range of (0−120%)		103
	PU-MXene nanoyarns		maximum sensing range: 208%, GF = 17−1730 at 20−208% strain, able to withstand 60% strain without any change in sensing relative resistance		108
	TPU/MXene/MWCNT		GF = 2911, broad working range of 330%	stable recovery after 2600 cycles of cyclic stretching at 50% strain	104
	PPy/MXene-PVDF		GF = 78−355.3, sensing range 0−100%		105
	MXene/GnP/CNC-SBS		54.9 S/m, GF = 400, ultralow detection limit of 0.25%, short response time (50 ms)	stable after 2000 cycles of loading−unloading at 100% strain	117
pressure sensors	$BaTiO_3$/MXene-PVDF-TrFE	piezoresistive	wide detection range (0.2−400 kPa), ultralow response of 56 ms	stable performance after 5000 compression cycles	61
	MXene-SF		high sensitivity of 298.4 kPa^{-1}, wide sensing range of up to 39.3 kPa	stable performance after 10,000 cycles of loading−unloading at 70% strain)	111
	MXene/ZIF-67/PAN		high sensitivity of 62.8 kPa^{-1}, a wide sensing range of up to100 kPa, and an outstanding recovery time of 10/8 ms	Stable performance after 10,000 cycles of loading−unloading	107
	PDMS/MXene-PVA	piezoresistive	a wide operating range (0−18 kPa), an ultrahigh sensitivity of 403.46 kPa^{-1}, a fast reaction time of 99.3 ms	remarkable durability after 12,000 pressure cycles	106
	MXene-PU/PAN/AgNW		high sensitivity (6.71 kPa^{-1}, 0.02−2 kPa^{-1}) and wide measurement range (0.02−700 kPa)		57
gas sensors	PVA/MXene/TiO2−CA	chemresistive	sensitivity toward NH3 (1−100 ppm) along with a fast response/recovery time (76 s/62 s) at room temperature		116
	PVA/PEI/MXene	chemresistive	high sensitivity (0.10−0.17 ppm−1), low experimental LOD (50 ppb), faster response−recovery (less than 2 min), and wide sensing range		112
	WS_2/MXene	chemresistive	response to NO2 (1 ppm) is 15.2%, limit of detection 11.0 ppb NO2, high stability under humidity		184
	V_2C MXene, polyester substrate	chemiresistive	response of 775% at 200 ppm toluene, good reproducibility, high selectivity, long-term stability	14 s/34 s	111
	$Ti_3C_2T_x$ MXene multilayers	chemiresistive	Limit of detection 250 ppb, fast response, high selectivity, excellent stability for 4 months	53 s (response)	185
self-powered sensors	MXene/PVA-$MoSe_2$	piezoelectric	shows high response of ∼40, fast response/recovery time of 0.9/6.3 s, low hysteresis of 1.8%, and stable repeatability		57
	MXene, styrene-ethylene-butylene-styrene (SEBS) substrate	triboelectric nanogenerators (TENG), pressure sensors, and multifunctional circuitry	power output ∼816.6 mW/mA^2, sensitivity ∼6.03, low detection limit ∼9 Pa	80 ms	186
	$Ti_3C_2T_x$ MXene/Ag nanocomposites	hybrid triboelectric-electromagnetic system	High response to ethanol (∼204% @ 100 ppm), voltage 581 V (TENG), 62 V (EMG)		187
	MXene/silicone nanocomposite	triboelectric effect with micropatterned surface	Peak power density 55.47 W/mA^2, voltage/current density improved by factors of 9.8 and 20		188
	MXene/black phosphorus (BP) lamellar structure	flexible pressure sensor, microsupercapacitors, and solar cells	Pressure sensitivity 77.61 kPa, high energy storage capacity, real-time detection of heart state	10.9 ms	189
electrochemical sensors	Fe-MOF/MXene nanocomposite	electrochemical (square wave anodic stripping voltammetry)	High sensitivity (8.94), limit of detection 0.58, strong As-hydroxyl bonding		190
	MXene-Cu_2O nanocomposite	electrochemical (chronoamperometry, cyclic voltammetry)	Broad linear range (0.01−30 mM), sensitivity 11.061, limit of detection 2.83 μM, high selectivity	short response time	191
	AuNPs@Ti_3C_2 MXene nanocomposite, silver ink on PET substrate	electrochemical (cyclic voltammetry)	real-time and label-free detection of 5 hmC, distinguishing 5 mC from 5 hmC, tumor detection capability		192
	MXene-based materials with surface functionalization/modification	electrochemical (bio)sensing for environmental contaminants	high selectivity and sensitivity for toxic elements, pharmaceutical residues, and pesticides		193

https://doi.org/10.1021/acsanm.5c02646
ACS Appl. Nano Mater. 2025, 8, 16231−16259

Table 3. continued

sensor type	composition	sensing mechanism	sensor performance	response/recovery time	reference
biosensors	Bromophenol blue (BPB)-delaminated Ti_3C_2 MXene, glucose oxidase (GO_x), luminol	electrochemiluminescent (ECL) reaction with luminol and H_2O_2	low detection limit (0.02), wide range (0.01−40,000 M), high sensitivity and selectivity		194
	MXene nanocomposites, enzymes, aptamers, DNA, immunoassays	electrochemical (microfluidic, wearable biosensors)	high sensitivity and selectivity, biomolecule immobilization, and future prospects for microfluidic and wearable sensors		195
	MXene-based materials with surface functionalization	electrochemical (bio)sensing for environmental pollutants	detection of toxic elements, pharmaceutical residues, and pesticides with high selectivity and sensitivity		193
	MXene hybridized with diversified nanomaterials	Lab-on-chip (LoC) biosensors integrated with AI, IoMT, 5G communication	on-site detection of biomarkers/pathogens, intelligent hospital-on-chip (HOC) solutions		196

sensitivity and often fail in humid environments. As for electrochemical sensors, the long-term stability of such devices is not sufficient for practical applications. Lastly, the breathability and wearability of such sensors are often overlooked in the studies, which makes it challenging to integrate them into real-world applications. Figure 14 illustrates the summary, challenges, and future research directions of MXene-based electrospun nanocomposites for flexible and wearable applications.

To mitigate the drawbacks faced by the MXene-based electrospun flexible sensors, several strategies could be realized. For example, a greener synthesis route should be employed for MXene synthesis. The synthesis process controls the defects and the lateral dimension of MXene nanosheets, which ultimately affects the sensor performance. It is speculated that more studies relating to the sustainable synthesis of MXenes will be focused on in the future. Currently, research on electrospun flexible sensors predominantly focuses on $Ti_3C_2T_x$ MXenes, with limited studies exploring other MXene compositions. It is anticipated that future research will focus on other MXene variants for flexible sensing applications beyond $Ti_3C_2T_x$. While most studies focus on single-nozzle electrospinning, it is speculated that more work will be reported on advanced electrospinning techniques such as coaxial electrospinning, near-field electrospinning, and 3D electrospinning to fabricate MXene-based nanocomposites. In addition, future efforts will be focused on combining artificial intelligence (AI)-driven smart flexible sensing technologies. Although the majority of studies investigate the fabrication and performance of flexible sensors, they do not adequately report on the safety and wearability aspects of flexible sensors. Hence, future endeavors will likely concentrate on the wearability and biocompatibility of wearable sensors.

Given their susceptibility to environmental oxidation, it is crucial to develop strategies to mitigate MXene degradation. Surface passivation using antioxidant molecules (e.g., ascorbic acid, tannic acid) or organic ligands can effectively suppress oxidation by forming a protective barrier against oxygen and moisture.[197] Polymer encapsulation, where MXenes are embedded within hydrophobic or semipermeable electrospun matrices (e.g., PVDF, TPU), can limit exposure to ambient conditions while preserving mechanical flexibility and signal responsiveness.[198] Additionally, controlled storage under inert atmospheres or refrigeration significantly delays oxidation during fabrication and handling. Advances in MXene synthesis, such as the MILD route or fluorine-free etching methods, also contribute to greater structural stability. Finally, hybridization with stable nanomaterials (e.g., graphene, carbon nanotubes) can create synergistic composites with enhanced durability and performance.[199−201] These strategies, individually or in combination, are promising paths to address future challenges related to the oxidation and environmental degradation of MXene-based electrospun sensors. Despite such progress, it is challenging to fully prevent MXenes from oxidizing. Future research should focus on the oxidation mechanism and prevent the partial/full oxidation of MXenes.

Long-term operational stability is essential for the practical deployment of MXene-based flexible sensors, particularly in wearable or continuous monitoring systems. Despite their excellent initial performance, MXene-based composites are susceptible to degradation under environmental stressors such as humidity, oxygen, mechanical fatigue, and temperature variations. Prolonged exposure often leads to oxidation,

https://doi.org/10.1021/acsanm.5c02646
ACS Appl. Nano Mater. 2025, 8, 16231−16259

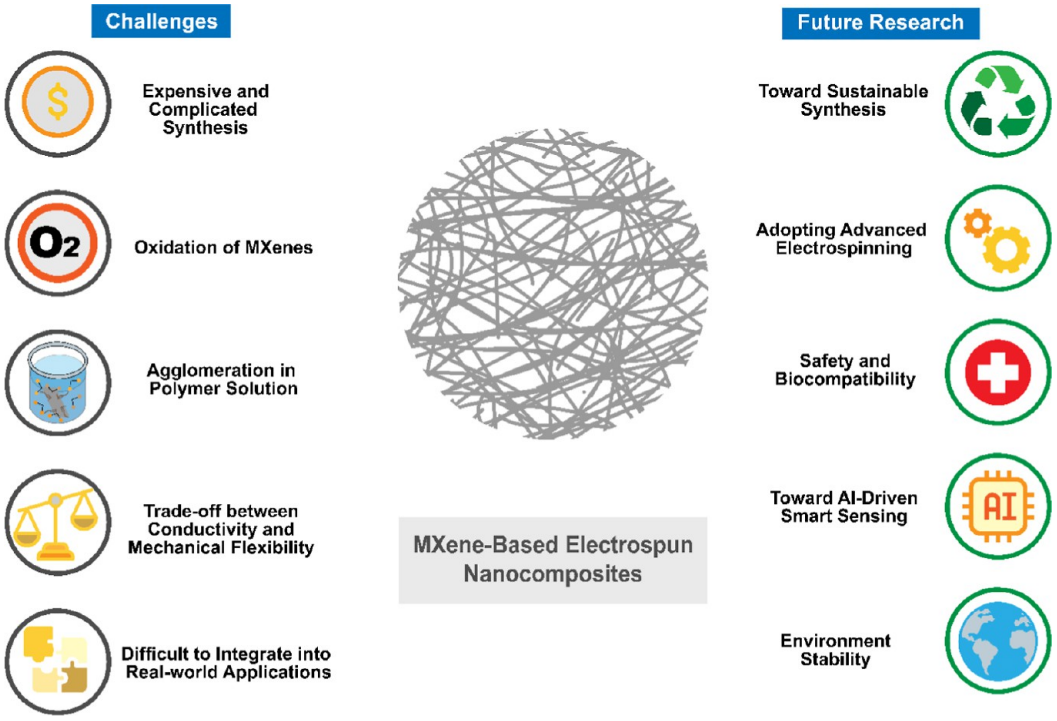

Figure 14. Contemporary challenges and future perspective of MXene-based electrospun nanocomposites for flexible and wearable sensing applications.

delamination, or loss of conductivity, compromising sensing reliability. Several studies have proposed strategies to mitigate these issues, including encapsulation with hydrophobic polymers, structural reinforcement using stable nanofillers (e.g., graphene), and chemical modification of MXenes to enhance resistance to ambient degradation.[123,150,202−204] Additionally, cyclic loading and fatigue tests are increasingly reported to evaluate mechanical and electrical durability over extended periods. While promising, more systematic and standardized stability assessments are needed across different sensing platforms. Emphasizing long-term reliability alongside sensitivity and selectivity is crucial for advancing MXene-based sensors toward commercial viability and real-world application.

The issues of biocompatibility and toxicity will be decisive in the question of the safe application of MXene-based flexible sensors in wearable applications.[205,206] Prolonged skin contact, exposure to bodily fluids, or implantation scenarios may pose risks due to potential ion leaching, oxidative degradation, or immune response. Functionalization of MXene surfaces with biocompatible polymers or coatings (e.g., PEG, chitosan) has been shown to improve safety profiles. However, long-term in vivo studies are still lacking, and regulatory approval pathways remain undeveloped. Comprehensive toxicological studies are essential before clinical or commercial deployment. Strategies include surface functionalization and rigorous biocompatibility assessments, and the researchers are working rigorously to make the entire loop more biocompatible. Meanwhile, improving the detection limits and selectivity of flexible MXene sensors requires further development of sensor design and detailed investigation of the complex interaction between the MXene-based electrospun composites and analytes. Despite current hurdles, MXene-based electrospun nanocomposites possess significant potential for widespread applications for designing next-generation wearable and flexible electronics. With continued research, flexible MXene-based electrospun nanocomposites could bridge the gap between lab-scale innovation and commercial adoption in healthcare, soft robotics, and smart textiles.

■ ASSOCIATED CONTENT

Data Availability Statement

Data will be made available on request.

Supporting Information

The Supporting Information is available free of charge at https://pubs.acs.org/doi/10.1021/acsanm.5c02646.

(ZIP)

■ AUTHOR INFORMATION

Corresponding Author

Habibur Rahman Anik − *Department of Chemistry and Chemical & Biomedical Engineering, University of New Haven, West Haven, Connecticut 06516, United States;* orcid.org/0000-0002-0609-8905; Email: habib15anik@gmail.com, hanik1@unh.newhaven.edu

Authors

Ashfaqul Hoque Khadem − *NanoBio Mechanics and Manufacturing Laboratory (NBM²), Department of Mechanical Engineering, College of Engineering, Computing, and Applied Science, Clemson University, Clemson, South Carolina 29634, United States; Department of Textile Engineering, University of Scholars, Dhaka 1213, Bangladesh*

Md Golam Mortuza Limon − *Department of Textile Engineering, University of Scholars, Dhaka 1213, Bangladesh*

Mahbubay Rabbani − *Department of Textile Engineering, University of Scholars, Dhaka 1213, Bangladesh*

Abu Sayed Rafi − *Department of Textile Engineering, University of Scholars, Dhaka 1213, Bangladesh*

https://doi.org/10.1021/acsanm.5c02646
ACS Appl. Nano Mater. 2025, 8, 16231−16259

Israt Khandaker Mim − *Department of Textile Engineering, University of Scholars, Dhaka 1213, Bangladesh*
Md Habibur Rahman − *Department of Textile Engineering, Uttara University, Dhaka 1230, Bangladesh*
Faisal Bin Alam − *Department of Textile Engineering, University of Scholars, Dhaka 1213, Bangladesh*
Md Khayrul Islam − *Department of Textile Engineering, University of Scholars, Dhaka 1213, Bangladesh*
Syeda Shirajum Munira − *Department of Textile Engineering, University of Scholars, Dhaka 1213, Bangladesh*
Md Touhidul Islam − *Department of Textile Engineering, University of Scholars, Dhaka 1213, Bangladesh*
Mohsin Uddin − *Department of Textile Engineering, University of Scholars, Dhaka 1213, Bangladesh; Department of Civil, Construction and Environmental Engineering, North Dakota State University, Fargo, North Dakota 58105, United States*
Hrishita Mony − *Department of Textile Engineering, University of Scholars, Dhaka 1213, Bangladesh*

Complete contact information is available at: https://pubs.acs.org/10.1021/acsanm.5c02646

Notes

The authors declare no competing financial interest.

REFERENCES

(1) Yan, Z.; Luo, S.; Li, Q.; Wu, Z. S.; Liu, S. F. Recent advances in flexible wearable supercapacitors: properties, fabrication, and applications. *Adv. Sci.* **2024**, *11* (8), 2302172.
(2) Quan, J.; Jiang, X.; Ding, T.; Ma, W.; Li, M.; Lan, C.; Xiang, H.; Li, W.; Zhu, M.; Zhang, Y. Recent progress in MXene fiber: Materials, fabrication techniques, and potential applications. *Chem. Eng. J.* **2025**, *503*, 158320.
(3) Chauhan, V. K.; Dubey, R.; Pandey, R.; Thennarasu, P.; Dubey, S. K. MXene on Textile Substrates: A Review. *Adv. Eng. Mater.* **2024**, *26* (7), 2301962.
(4) Anik, H. R.; Tushar, S. I.; Mahmud, S.; Khadem, A. H.; Sen, P.; Akter, M. Into the Revolution of NanoFusion: Merging High Performance and Aesthetics by Nanomaterials in Textile Finishes. *Adv. Mater. Interfaces* **2025**, *12* (1), 2400368.
(5) Verma, R.; Thakur, P.; Chauhan, A.; Jasrotia, R.; Thakur, A. A review on MXene and its' composites for electromagnetic interference (EMI) shielding applications. *Carbon* **2023**, *208*, 170−190.
(6) Anasori, B.; Naguib, M. Two-dimensional MXenes. *MRS Bull.* **2023**, *48* (3), 238−244.
(7) Otgonbayar, Z.; Oh, W. C. Comprehensive and multi-functional MXene based sensors: An updated review. *FlatChem* **2023**, *40*, 100524.
(8) Levitt, A.; Zhang, J.; Dion, G.; Gogotsi, Y.; Razal, J. M. MXene-Based Fibers, Yarns, and Fabrics for Wearable Energy Storage Devices. *Adv. Funct. Mater.* **2020**, *30* (47), 2000739.
(9) Khadem, A. H.; Hasan, T. U.; Rahman, A. N. M. M.; Smriti, S. A.; Alimuzzaman, S. Fabrication, properties, and performance of graphene-based textile fabrics for supercapacitor applications: A review. *J. Energy Storage* **2022**, *56*, 105988.
(10) Khadem, A. H. Recent Advances in Functional Fabric-Based Wearable Supercapacitors. *Adv. Mater. Interfaces* **2024**, *11* (7), 2300724.
(11) Kannan, K.; Sadasivuni, K. K.; Abdullah, A. M.; Kumar, B. Current Trends in MXene-Based Nanomaterials for Energy Storage and Conversion System: A Mini Review. *Catalysts* **2020**, *10*, 495.
(12) Song, P.; Liu, B.; Qiu, H.; Shi, X.; Cao, D.; Gu, J. MXenes for polymer matrix electromagnetic interference shielding composites: A review. *Compos. Commun.* **2021**, *24*, 100653.
(13) Khan, K.; Tareen, A. K.; Iqbal, M.; Ye, Z.; Xie, Z.; Mahmood, A.; Mahmood, N.; Zhang, H. J. S. Recent progress in emerging novel MXenes based materials and their fascinating sensing applications. *Small* **2023**, *19* (19), 2206147.
(14) Riazi, H.; Taghizadeh, G.; Soroush, M. MXene-Based Nanocomposite Sensors. *ACS Omega* **2021**, *6* (17), 11103−11112.
(15) Iakunkov, A.; Lienert, U.; Sun, J.; Talyzin, A. V. Swelling of Ti3C2Tx MXene in Water and Methanol at Extreme Pressure Conditions. *Adv. Sci.* **2024**, *11* (9), 2307067.
(16) Ran, L.; Qiu, L.; Zhao, H.; Sun, F.; Chen, Z.; Zhao, L.; Yi, L.; Ji, X. M. Fabrication of MXene based sandwich-like films for excellent flexibility, electromagnetic interference shielding and thermal management. *Composites, Part A* **2023**, *173*, 107672.
(17) Chen, R.; Jia, X.; Zhou, H.; Ren, S.; Han, D.; Li, S.; Gao, Z. Applications of MXenes in wearable sensing: Advances, challenges, and prospects. *Mater. Today* **2024**, *75*, 359−385.
(18) Cao, W.; Nie, J.; Cao, Y.; Gao, C.; Wang, M.; Wang, W.; Lu, X.; Ma, X.; Zhong, P. A review of how to improve Ti3C2Tx MXene stability. *Chem. Eng. J.* **2024**, *496*, 154097.
(19) Zhou, Y.; Zhang, Y.; Ruan, K.; Guo, H.; He, M.; Qiu, H.; Gu, J. MXene-based fibers: Preparation, applications, and prospects. *Sci. Bull.* **2024**, *69* (17), 2776−2792.
(20) Bai, W.; Shi, L.; Li, Z.; Liu, D.; Liang, Y.; Han, B.; Qi, J.; Li, Y. Recent progress on the preparation and application in photocatalysis of 2D MXene-based materials. *Mater. Today Energy* **2024**, *41*, 101547.
(21) Jianxin, L.; Xuedi, C.; Xiaolei, Z.; Xicheng, J.; Hengzhe, Y.; Junlin, F. Review on functional electrospun nanofibers: Theory, application and fabrication. *Mater. Sci. Eng., B* **2024**, *307*, 117488.
(22) Olmedo-Pradas, J.; Gañán-Calvo, A. M.; Modesto-López, L. B. Integrating a micro-mixing mechanism and on-line thermal processing for the large-scale ejection of polymeric liquid threads for producing ultrafine fibers. *RSC Adv.* **2023**, *13* (27), 18511−18524.
(23) Serrano-Garcia, W.; Bonadies, I.; Thomas, S. W.; Guarino, V. New Insights to Design Electrospun Fibers with Tunable Electrical Conductive−Semiconductive Properties. *Sensors* **2023**, *23* (3), 1606.
(24) Das, P.; Ganguly, S.; Rosenkranz, A.; Wang, B.; Yu, J.; Srinivasan, S.; Rajabzadeh, A. R. MXene/0D nanocomposite architectures: Design, properties and emerging applications. *Mater. Today Nano* **2023**, *24*, 100428.
(25) Wang, Y.; Adam, M. L.; Zhao, Y.; Zheng, W.; Gao, L.; Yin, Z.; Zhao, H. Machine learning-enhanced flexible mechanical sensing. *Nano-Micro Lett.* **2023**, *15* (1), 55.
(26) Yu, L.; Chen, L.; Liu, Y.; Zhu, J.; Wang, F.; Ma, L.; Yi, K.; Xiao, H.; Zhou, F.; Wang, F.; Bai, L.; Zhu, Y.; Xiao, X.; Yang, Y. Magnetically Actuated Hydrogel Stamping-Assisted Cellular Mechanical Analyzer for Stored Blood Quality Detection. *ACS Sens.* **2023**, *8* (3), 1183−1191.
(27) Huang, C.-Y.; Yang, G.; Huang, P.; Hu, J.-M.; Tang, Z.-H.; Li, Y.-Q.; Fu, S.-Y. Flexible pressure sensor with an excellent linear response in a broad detection range for human motion monitoring. *ACS Appl. Mater. Interfaces* **2023**, *15* (2), 3476−3485.
(28) Gao, F.-L.; Liu, J.; Li, X.-P.; Ma, Q.; Zhang, T.; Yu, Z.-Z.; Shang, J.; Li, R.-W.; Li, X. Ti3C2Tx MXene-Based Multifunctional Tactile Sensors for Precisely Detecting and Distinguishing Temperature and Pressure Stimuli. *ACS Nano* **2023**, *17* (16), 16036−16047.
(29) Coatsworth, P.; Gonzalez-Macia, L.; Collins, A. S. P.; Bozkurt, T.; Güder, F. Continuous monitoring of chemical signals in plants under stress. *Nat. Rev. Chem.* **2023**, *7* (1), 7−25.
(30) Wang, Z.; Wei, H.; Huang, Y.; Wei, Y.; Chen, J. Naturally sourced hydrogels: emerging fundamental materials for next-generation healthcare sensing. *Chem. Soc. Rev.* **2023**, *52* (9), 2992−3034.
(31) Maity, C. K.; De, S.; De Adhikari, A.; Kumari, A.; Verma, K.; Moniruzzaman, M.; Sahoo, S. Impact of 3D printed MXene electrodes on energy storage: Different dimensionalities, electrochemistry and performance optimization of printable MXene ink. *Energy Storage Mater.* **2024**, *73*, 103873.
(32) Matias, M. L.; Pereira, C.; Almeida, H. V.; Jana, S.; Panigrahi, S.; Menda, U. D.; Nunes, D.; Fortunato, E.; Martins, R.; Nandy, S. 3D printed MXene architectures for a plethora of smart applications. *Mater. Today Adv.* **2024**, *23*, 100512.
(33) Mercante, L. A.; Andre, R. S.; Facure, M. H.; Correa, D. S.; Mattoso, L. H. C. Recent progress in conductive electrospun materials for flexible electronics: Energy, sensing, and electromagnetic shielding applications. *Chem. Eng. J.* **2023**, *465*, 142847.

(34) Li, F.; Zhao, S.; Wang, H.; Zhu, G.; Li, H. MXene Fibers for Flexible and Wearable Electronics: Recent Progress and Future Perspectives. *Chem.—Asian J.* **2023**, *18* (16), No. e202300474.
(35) Khademolqorani, S.; Banitaba, S. N.; Gupta, A.; Poursharifi, N.; Ghaffari, A. A.; Jadhav, V. V.; Arifeen, W. U.; Singh, M.; Borah, M.; Chamanehpour, E.; Mishra, Y. K. Application Scopes of Miniaturized MXene-Functionalized Electrospun Nanofibers-Based Electrochemical Energy Devices. *Small* **2023**, *20*, 2309572.
(36) Lim, K. R. G.; Shekhirev, M.; Wyatt, B. C.; Anasori, B.; Gogotsi, Y.; Seh, Z. W. Fundamentals of MXene synthesis. *Nat. Synth.* **2022**, *1* (8), 601−614.
(37) Alhabeb, M.; Maleski, K.; Anasori, B.; Lelyukh, P.; Clark, L.; Sin, S.; Gogotsi, Y. Guidelines for Synthesis and Processing of Two-Dimensional Titanium Carbide (Ti3C2Tx MXene). *Chem. Mater.* **2017**, *29* (18), 7633−7644.
(38) Kim, Y.-J.; Kim, S. J.; Seo, D.; Chae, Y.; Anayee, M.; Lee, Y.; Gogotsi, Y.; Ahn, C. W.; Jung, H.-T. Etching Mechanism of Monoatomic Aluminum Layers during MXene Synthesis. *Chem. Mater.* **2021**, *33* (16), 6346−6355.
(39) Persson, P. O. Å.; Rosen, J. Current state of the art on tailoring the MXene composition, structure, and surface chemistry. *Curr. Opin. Solid State Mater. Sci.* **2019**, *23* (6), 100774.
(40) Qureshi, A.; Abdelhay, A. H.; Zaidi, S. A.; Tariq, H.; Sadasivuni, K. K.; Sheikh, H.; Mohamed, M. Emerging trends in niobium, vanadium, and molybdenum based MXenes applications. *Crit. Rev. Solid State Mater. Sci.* **2024**, *49* (1), 141−162.
(41) Jin, S.; Guo, Y.; Wang, F.; Zhou, A. The synthesis of MXenes. *MRS Bull.* **2023**, *48* (3), 245−252.
(42) Naguib, M.; Kurtoglu, M.; Presser, V.; Lu, J.; Niu, J.; Heon, M.; Hultman, L.; Gogotsi, Y.; Barsoum, M. W. Two-Dimensional Nanocrystals Produced by Exfoliation of Ti3AlC2. *Adv. Mater.* **2011**, *23* (37), 4248−4253.
(43) Wei, Y.; Zhang, P.; Soomro, R. A.; Zhu, Q.; Xu, B. Advances in the Synthesis of 2D MXenes. *Adv. Mater.* **2021**, *33* (39), 2103148.
(44) Anjum, N.; Rahman, M. M.; Elattar, A.; Sijuade, A.; Kalu, E. E.; Okoli, O. I. High-Yield MILD Synthesis of Ti3C2Tx MXene: Characterization and Application in Developing Energy Storage Device. *Adv. Sustainable Syst.* **2025**, 2500402.
(45) Sun, W.; Shah, S. A.; Chen, Y.; Tan, Z.; Gao, H.; Habib, T.; Radovic, M.; Green, M. J. Electrochemical etching of Ti2AlC to Ti2CTx (MXene) in low-concentration hydrochloric acid solution. *J. Mater. Chem. A* **2017**, *5* (41), 21663−21668.
(46) Li, G.; Tan, L.; Zhang, Y.; Wu, B.; Li, L. Highly Efficiently Delaminated Single-Layered MXene Nanosheets with Large Lateral Size. *Langmuir* **2017**, *33* (36), 9000−9006.
(47) Li, M.; Lu, J.; Luo, K.; Li, Y.; Chang, K.; Chen, K.; Zhou, J.; Rosen, J.; Hultman, L.; Eklund, P.; Persson, P. O. Å.; Du, S.; Chai, Z.; Huang, Z.; Huang, Q. Element Replacement Approach by Reaction with Lewis Acidic Molten Salts to Synthesize Nanolaminated MAX Phases and MXenes. *J. Am. Chem. Soc.* **2019**, *141* (11), 4730−4737.
(48) Kamysbayev, V.; Filatov, A. S.; Hu, H.; Rui, X.; Lagunas, F.; Wang, D.; Klie, R. F.; Talapin, D. V. Covalent surface modifications and superconductivity of two-dimensional metal carbide MXenes. *Science* **2020**, *369* (6506), 979−983.
(49) Mashtalir, O.; Naguib, M.; Mochalin, V. N.; Dall'Agnese, Y.; Heon, M.; Barsoum, M. W.; Gogotsi, Y. Intercalation and delamination of layered carbides and carbonitrides. *Nat. Commun.* **2013**, *4* (1), 1716.
(50) Liu, F.; Zhou, A.; Chen, J.; Jia, J.; Zhou, W.; Wang, L.; Hu, Q. Preparation of Ti3C2 and Ti2C MXenes by fluoride salts etching and methane adsorptive properties. *Appl. Surf. Sci.* **2017**, *416*, 781−789.
(51) Halim, J.; Kota, S.; Lukatskaya, M. R.; Naguib, M.; Zhao, M.-Q.; Moon, E. J.; Pitock, J.; Nanda, J.; May, S. J.; Gogotsi, Y.; Barsoum, M. W. Synthesis and Characterization of 2D Molybdenum Carbide (MXene). *Adv. Funct. Mater.* **2016**, *26* (18), 3118−3127.
(52) Naguib, M.; Unocic, R. R.; Armstrong, B. L.; Nanda, J. Large-scale delamination of multi-layers transition metal carbides and carbonitrides "MXenes". *Dalton Trans.* **2015**, *44* (20), 9353−9358.
(53) Cao, F.; Zhang, Y.; Wang, H.; Khan, K.; Tareen, A. K.; Qian, W.; Zhang, H.; Ågren, H. Recent Advances in Oxidation Stable Chemistry of 2D MXenes. *Adv. Mater.* **2022**, *34* (13), 2107554.
(54) Habib, T.; Zhao, X.; Shah, S. A.; Chen, Y.; Sun, W.; An, H.; Lutkenhaus, J. L.; Radovic, M.; Green, M. J. Oxidation stability of Ti3C2Tx MXene nanosheets in solvents and composite films. *npj 2D Mater. Appl.* **2019**, *3* (1), 8.
(55) Mayerberger, E. A.; Urbanek, O.; McDaniel, R. M.; Street, R. M.; Barsoum, M. W.; Schauer, C. L. Preparation and characterization of polymer-$Ti_3C_2T_x$ (MXene) composite nanofibers produced via electrospinning. *J. Appl. Polym. Sci.* **2017**, *134* (37), 45295.
(56) Sobolčiak, P.; Tanvir, A.; Sadasivuni, K. K.; Krupa, I. Piezoresistive Sensors Based on Electrospun Mats Modified by 2D Ti3C2Tx MXene. *Sensors* **2019**, *19*, 4589.
(57) Wang, D.; Zhang, D.; Li, P.; Yang, Z.; Mi, Q.; Yu, L. Electrospinning of Flexible Poly(vinyl alcohol)/MXene Nanofiber-Based Humidity Sensor Self-Powered by Monolayer Molybdenum Diselenide Piezoelectric Nanogenerator. *Nano-Micro Lett.* **2021**, *13* (1), 57.
(58) Al-Dhahebi, A. M.; Jose, R.; Mustapha, M.; Saheed, M. S. M. Ultrasensitive aptasensor using electrospun MXene/polyvinylidene fluoride nanofiber composite for Ochratoxin A detection. *Food Chem.* **2022**, *390*, 133105.
(59) Liu, Y.; Wang, H.; Zhao, W.; Zhang, M.; Qin, H.; Xie, Y. Flexible, Stretchable Sensors for Wearable Health Monitoring: Sensing Mechanisms, Materials, Fabrication Strategies and Features. *Sensors* **2018**, *18*, 645.
(60) Aabdin, Z.; Peranio, N.; Winkler, M.; Bessas, D.; König, J.; Hermann, R. P.; Böttner, H.; Eibl, O. Sb2Te3 and Bi2Te3 Thin Films Grownby Room-Temperature MBE. *J. Electron. Mater.* **2012**, *41* (6), 1493−1497.
(61) Liu, X.; Tong, J.; Wang, J.; Lu, S.; Yang, D.; Li, H.; Liu, C.; Song, Y. BaTiO3/MXene/PVDF-TrFE composite films via an electrospinning method for flexible piezoelectric pressure sensors. *J. Mater. Chem. C* **2023**, *11* (14), 4614−4622.
(62) Wang, G.; Meng, L.; Ji, X.; Liu, X.; Liang, J.; Liu, S. Nacre-inspired MXene-based film for highly sensitive piezoresistive sensing over a broad sensing range. *BDM* **2024**, *7* (4), 463−475.
(63) Yang, N.; Yin, X.; Liu, H.; Zhou, X.; Yan, X.; Zhao, Y.; Cheng, T. High-Performance Wearable Piezoresistive Sensor with a Wide Temperature Range via a Ti3C2Tx MXene/Au Dual-Layer Conductive Network and Microspike Structure. *ACS Appl. Nano Mater.* **2024**, *7* (14), 16964−16974.
(64) Du, C.; Zhang, H.; Liu, X.; Zhou, S.; Ma, Y.; Li, S.; Zhang, Y. Flexible and Simply Degradable MXene−Methylcellulose Piezoresistive Sensor for Human Motion Detection. *ACS Appl. Mater. Interfaces* **2024**, *16* (10), 12996−13005.
(65) Ge, C.; Sun, B.; Huang, Y.; Alahi, M. E. E.; Ma, Q.; Wei, S.; Hui, Y.; Huang, Z.; Zeng, Q. Recent Advances in Multi-Scale Piezoresistive Interfaces for MXene-Based Flexible Sensors. *Adv. Mater. Technol.* **2024**, *9* (8), 2301897.
(66) Chen, J.; Song, T.; Wang, X.; Zhou, Y.; Wang, T.; Zhang, X.; Zhao, Y.; Yang, B.; Zhang, Y.; Chen, J.; Chen, K.; Li, Y.; Han, W. Ultrasensitive and wide-range MXene/PDMS piezoresistive sensors inspired by rose petals. *Nano Energy* **2024**, *131*, 110285.
(67) Jin, L.; Ao, Y.; Xu, T.; Zou, Y.; Yang, W. Recent advances in MXene-based composites for piezoelectric sensors. *Nanoscale* **2024**, *16* (47), 21673−21696.
(68) Zhang, X.; Wang, Y.; Zhang, L.; Zhang, X.; Guo, Y.; Hao, B.; Qin, Y.; Li, Q.; Fan, L.; Dong, H.; Tan, Q. Facile preparation of porous MXene/cellulose nanofiber composite for highly-sensitive flexible piezoresistive sensors in e-skin. *Chem. Eng. J.* **2025**, *505*, 159369.
(69) He, X.; Zhang, L.; Lu, X.; Zhang, A.; Zhang, J. Carboxymethyl Chitosan Synergistically Enhanced MXene Composite Aerogel for Piezoresistive Sensors and Thermal Management. *Ind. Eng. Chem. Res.* **2024**, *63* (36), 15901−15911.
(70) Zhang, H.; Du, C.; Zhang, Y. Constructing the 3D Interconnected Conductive MXene-Cellulose Scaffold to Boosting

the Piezoresistive Sensing Capability. *ACS Appl. Electron. Mater.* **2024**, *6* (9), 6785−6792.
(71) Cheng, H.; Zhang, L.; Feng, J.; Tang, T.; Qin, D. A novel sensor based on Ti3C2MXene/Co3O4/carbon nanofibers composite for the sensitive detection of 4-aminophenol. *Chemosphere* **2023**, *341*, 139981.
(72) Jiang, Y.; Wu, L.; Chen, Q.; Li, N.; Tian, J. High-performance capacitive humidity sensor based on flower-like SnS2/Ti3C2MXene for respiration monitoring and non-contact sensing. *Sens. Actuators, B* **2025**, *426*, 137012.
(73) Cui, X.; Zheng, J.; Huang, Y.; Wang, R.; Zhang, H. MXene/MWCNTs-based capacitive pressure sensors combine high sensitivity and wide detection range for human health and motion monitoring. *Sens. Actuators, A* **2024**, *379*, 115858.
(74) Ji, K.; Liang, Z.; Wang, P.; Li, Z.; Ma, Q.; Su, X. Mxene-based capacitive enzyme-free biofuel cell Self-Powered sensor for lead ion detection in human plasma. *Chem. Eng. J.* **2024**, *495*, 153598.
(75) Zheng, Z.; Fang, X.; Pan, Y.; Song, S.; Xue, H.; Li, J.; Li, Y.; Li, J. A liquid metal-embedded 3D interconnected-porous TPU/MXene composite with improved capacitive sensitivity and pressure detection range. *RSC Adv.* **2024**, *14* (22), 15730−15741.
(76) Du, H.; Zhou, H.; Wang, M.; Zhao, G.; Jin, X.; Liu, H.; Chen, W.; Weng, W.; Ma, A. Electrospun Elastic Films Containing AgNW-Bridged MXene Networks as Capacitive Electronic Skins. *ACS Appl. Mater. Interfaces* **2022**, *14* (27), 31225−31233.
(77) Zhang, L.; Zhang, S.; Wang, C.; Zhou, Q.; Zhang, H.; Pan, G.-B. Highly Sensitive Capacitive Flexible Pressure Sensor Based on a High-Permittivity MXene Nanocomposite and 3D Network Electrode for Wearable Electronics. *ACS Sens.* **2021**, *6* (7), 2630−2641.
(78) Fang, X.; Song, Y.; Huang, Y.; Yang, G.; Han, C.; Li, H.; Qu, L. Two-dimensional MXene modified AgNRs as a surface-enhanced Raman scattering substrate for sensitive determination of polychlorinated biphenyls. *Analyst* **2020**, *145* (22), 7421−7428.
(79) Baig, M. M.; Saqib, Q. M.; Noman, M.; Sheeraz, M.; Rasheed, A.; Yousuf, M.; Lee, E.; Kim, J.; Ko, Y.; Patil, C. S.; Patil, S. R.; Ju, H.; Lee, S. G.; et al. Novel Intercalation Approach in MXene Using Modified Silica Nanospheres to Enhance the Surface Charge Density for Superior Triboelectric Performance. *Adv. Funct. Mater.* **2024**, *34* (48), 2408271.
(80) Liu, B.; Zhang, X.; Li, B.; Zhang, X. Interfacial dielectric enhancement in MXene/PVDF nanocomposites via hydrogen bond-induced dipole modulation. *Appl. Surf. Sci.* **2025**, *695*, 162837.
(81) Faruk, O.; Islam, M. R.; Rana, S. M. S.; Pradhan, G. B.; Kim, H.; Asaduzzaman, M.; Bhatta, T.; Park, J. Y. V2CTX-MXene-functionalized fluoropolymer composite nanofibrous mat-based high-performance triboelectric nanogenerator for self-powered human activity and posture monitoring. *Nano Energy* **2024**, *127*, 109787.
(82) Tan, D.; Jiang, C.; Sun, N.; Huang, J.; Zhang, Z.; Zhang, Q.; Bu, J.; Bi, S.; Guo, Q.; Song, J. Piezoelectricity in monolayer MXene for nanogenerators and piezotronics. *Nano Energy* **2021**, *90*, 106528.
(83) Wang, S.; Shao, H.-Q.; Liu, Y.; Tang, C.-Y.; Zhao, X.; Ke, K.; Bao, R.-Y.; Yang, M.-B.; Yang, W. Boosting piezoelectric response of PVDF-TrFE via MXene for self-powered linear pressure sensor. *Compos. Sci. Technol.* **2021**, *202*, 108600.
(84) Huang, Y.; Chen, S.; Li, Y.; Lin, Q.; Wu, Y.; Shi, Q. Flexible piezoelectric sensor based on PAN/MXene/PDA@ZnO composite film for human health and motion detection with fast response and highly sensitive. *Chem. Eng. J.* **2024**, *488*, 150997.
(85) Zhang, J.; Wang, Z.; Huang, Y.; Pi, X.; Wu, Y.; Shi, Q. Flexible piezoelectric sensor based on polyacrylonitrile/MWCNT/MXene composites films for human physiological health detection. *J. Appl. Polym. Sci.* **2024**, *141* (9), No. e55009.
(86) Pan, H.; Lee, T.-W. Recent Progress in Development of Wearable Pressure Sensors Derived from Biological Materials. *Adv. Healthcare Mater.* **2021**, *10* (17), 2100460.
(87) Niu, S.; Liu, Y.; Wang, S.; Lin, L.; Zhou, Y. S.; Hu, Y.; Wang, Z. L. Theoretical Investigation and Structural Optimization of Single-Electrode Triboelectric Nanogenerators. *Adv. Funct. Mater.* **2014**, *24* (22), 3332−3340.
(88) Bhatta, T.; Maharjan, P.; Cho, H.; Park, C.; Yoon, S. H.; Sharma, S.; Salauddin, M.; Rahman, M. T.; Rana, S. M. S.; Park, J. Y. High-performance triboelectric nanogenerator based on MXene functionalized polyvinylidene fluoride composite nanofibers. *Nano Energy* **2021**, *81*, 105670.
(89) Chaudhary, V.; Ashraf, N.; Khalid, M.; Walvekar, R.; Yang, Y.; Kaushik, A.; Mishra, Y. K. Emergence of MXene−Polymer Hybrid Nanocomposites as High-Performance Next-Generation Chemiresistors for Efficient Air Quality Monitoring. *Adv. Funct. Mater.* **2022**, *32* (33), 2112913.
(90) Kannan, K.; Sliem, M. H.; Abdullah, A. M.; Sadasivuni, K. K.; Kumar, B. Fabrication of ZnO-Fe-MXene Based Nanocomposites for Efficient CO2 Reduction. *Catalysts* **2020**, *10*, 549.
(91) Yu, H.; Dai, L.; Liu, Y.; Zhou, Y.; Fan, P.; Luo, J.; Zhong, A. Ti3C2Tx MXene-SnO2 nanocomposite for superior room temperature ammonia gas sensor. *J. Alloys Compd.* **2023**, *962*, 171170.
(92) Tian, G.; Xu, K.; Huang, Y.; You, X.; Yu, W.; Liu, H.; Li, J.; Liu, J.; Jin, X.; Li, H.; Ke, Q.; Huang, C. An organic/inorganic coating strategy that greatly enhanced sensing performances and reliability of all-fabric piezoresistive sensors. *J. Mater. Chem. A* **2023**, *11* (39), 21333−21344.
(93) Zhou, Y.; Zhao, L.; Tao, W.; Wang, T.; Sun, P.; Liu, F.; Yan, X.; Lu, G. All-Nanofiber Network Structure for Ultrasensitive Piezoresistive Pressure Sensors. *ACS Appl. Mater. Interfaces* **2022**, *14* (17), 19949−19957.
(94) Cuthbert, T. J.; Hannigan, B. C.; Roberjot, P.; Shokurov, A. V.; Menon, C. HACS: Helical Auxetic Yarn Capacitive Strain Sensors with Sensitivity Beyond the Theoretical Limit. *Adv. Mater.* **2023**, *35* (10), 2209321.
(95) Zhang, M.; Gu, M.; Shao, L.; Cheng, G.; Gao, H.; Sun, B.; Li, S.; Tang, T.; Li, N.; Yi, Y.; Wei, D.; Yang, C.; Wei, D. Flexible Wearable Capacitive Sensors Based on Ionic Gel with Full-Pressure Ranges. *ACS Appl. Mater. Interfaces* **2023**, *15* (12), 15884−15892.
(96) Hossain, I. Z.; Khan, A.; Hossain, G. A Piezoelectric Smart Textile for Energy Harvesting and Wearable Self-Powered Sensors. *Energies* **2022**, *15* (15), 5541.
(97) Zhou, Z.; Zhang, Q.; Zhang, Z.; Kuang, H.; Du, X.; Yang, H. Lead-free, high-current output piezoelectric nanogenerators using three-dimensional interdigitated electrodes. *Chem. Eng. J.* **2022**, *442*, 136241.
(98) Wu, Y.; Cui, X.; Wu, H.; Su, Z. All-polymeric fibrous triboelectric nanogenerator for self-powered intelligent active motions monitoring system. *Chem. Eng. J.* **2023**, *469*, 143708.
(99) Yu, Y.; Gao, Q.; Zhang, X.; Zhao, D.; Xia, X.; Wang, J.; Li, H.; Wang, Z. L.; Cheng, T. Contact-sliding-separation mode triboelectric nanogenerator. *Energy Environ. Sci.* **2023**, *16* (9), 3932−3941.
(100) Rath, R. J.; Farajikhah, S.; Oveissi, F.; Dehghani, F.; Naficy, S. Chemiresistive Sensor Arrays for Gas/Volatile Organic Compounds Monitoring: A Review. *Adv. Eng. Mater.* **2023**, *25* (3), 2200830.
(101) Tang, R.; Shi, Y.; Hou, Z.; Wei, L. Carbon Nanotube-Based Chemiresistive Sensors. *Sensors* **2017**, *17*, 882.
(102) Mayerberger, E. A.; Street, R. M.; McDaniel, R. M.; Barsoum, M. W.; Schauer, C. L. Antibacterial properties of electrospun Ti3C2Tz (MXene)/chitosan nanofibers. *RSC Adv.* **2018**, *8* (62), 35386−35394.
(103) Li, X.; Yang, J.; Yuan, W.; Ji, P.; Xu, Z.; Shi, S.; Han, X.; Niu, W.; Yin, F. Microstructured MXene/polyurethane fibrous membrane for highly sensitive strain sensing with ultra-wide and tunable sensing range. *Compos. Commun.* **2021**, *23*, 100586.
(104) Dong, H.; Sun, J.; Liu, X.; Jiang, X.; Lu, S. Highly Sensitive and Stretchable MXene/CNTs/TPU Composite Strain Sensor with Bilayer Conductive Structure for Human Motion Detection. *ACS Appl. Mater. Interfaces* **2022**, *14* (13), 15504−15516.
(105) Leong, W. X.; Al-Dhahebi, A. M.; Ahmad, M. R.; Saheed, M. S. Ti3C2Tx MXene-Polymeric Strain Sensor with Huge Gauge Factor for Body Movement Detection. *Micromachines* **2022**, *13*, 1302.
(106) Yan, J.; Ma, Y.; Jia, G.; Zhao, S.; Yue, Y.; Cheng, F.; Zhang, C.; Cao, M.; Xiong, Y.; Shen, P.; Gao, Y. Bionic MXene based hybrid film design for an ultrasensitive piezoresistive pressure sensor. *Chem. Eng. J.* **2022**, *431*, 133458.
(107) Fu, X.; Li, J.; Li, D.; Zhao, L.; Yuan, Z.; Shulga, V.; Han, W.; Wang, L. MXene/ZIF-67/PAN Nanofiber Film for Ultra-sensitive

Pressure Sensors. *ACS Appl. Mater. Interfaces* **2022**, *14* (10), 12367−12374.
(108) Levitt, A.; Seyedin, S.; Zhang, J.; Wang, X.; Razal, J. M.; Dion, G.; Gogotsi, Y. Bath Electrospinning of Continuous and Scalable Multifunctional MXene-Infiltrated Nanoyarns. *Small* **2020**, *16* (26), 2002158.
(109) Gao, X.; Li, Z.-K.; Xue, J.; Qian, Y.; Zhang, L.-Z.; Caro, J.; Wang, H. Titanium carbide Ti3C2Tx (MXene) enhanced PAN nanofiber membrane for air purification. *J. Membr. Sci.* **2019**, *586*, 162−169.
(110) Fang, F.; Wang, H.; Wang, H.; Gu, X.; Zeng, J.; Wang, Z.; Chen, X.; Chen, X.; Chen, M. Stretchable MXene/Thermoplastic Polyurethanes based Strain Sensor Fabricated Using a Combined Electrospinning and Electrostatic Spray Deposition Technique. *Micromachines* **2021**, *12*, 252.
(111) Chao, M.; He, L.; Gong, M.; Li, N.; Li, X.; Peng, L.; Shi, F.; Zhang, L.; Wan, P. Breathable Ti3C2Tx MXene/Protein Nanocomposites for Ultrasensitive Medical Pressure Sensor with Degradability in Solvents. *ACS Nano* **2021**, *15* (6), 9746−9758.
(112) Yuan, W.; Yang, K.; Peng, H.; Li, F.; Yin, F. A flexible VOCs sensor based on a 3D Mxene framework with a high sensing performance. *J. Mater. Chem. A* **2018**, *6* (37), 18116−18124.
(113) Awasthi, G. P.; Maharjan, B.; Shrestha, S.; Bhattarai, D. P.; Yoon, D.; Park, C. H.; Kim, C. S. Synthesis, characterizations, and biocompatibility evaluation of polycaprolactone−MXene electrospun fibers. *Colloids Surf., A* **2020**, *586*, 124282.
(114) Nguyen, T. D.; Roh, S.; Nguyen, M. T. N.; Lee, J. S. Structural Control of Nanofibers According to Electrospinning Process Conditions and Their Applications. *Micromachines* **2023**, *14* (11), 2022.
(115) Song, J.; Lin, X.; Ee, L. Y.; Li, S. F. Y.; Huang, M. A review on electrospinning as versatile supports for diverse nanofibers and their applications in environmental sensing. *Adv. Fiber Mater.* **2023**, *5* (2), 429−460.
(116) Sardana, S.; Kaur, H.; Arora, B.; Aswal, D. K.; Mahajan, A. Self-Powered Monitoring of Ammonia Using an MXene/TiO2/Cellulose Nanofiber Heterojunction-Based Sensor Driven by an Electrospun Triboelectric Nanogenerator. *ACS Sens.* **2022**, *7* (1), 312−321.
(117) Mohseni Taromsari, S.; Shi, H. H.; Saadatnia, Z.; Park, C. B.; Naguib, H. E. Design and development of ultra-sensitive, dynamically stable, multi-modal GnP@MXene nanohybrid electrospun strain sensors. *Chem. Eng. J.* **2022**, *442*, 136138.
(118) Rogers, J. A.; Someya, T.; Huang, Y. Materials and mechanics for stretchable electronics. *Science* **2010**, *327* (5973), 1603−1607.
(119) Zheng, X.; Wang, P.; Zhang, X.; Hu, Q.; Wang, Z.; Nie, W.; Zou, L.; Li, C.; Han, X. Breathable, durable and bark-shaped MXene/textiles for high-performance wearable pressure sensors, EMI shielding and heat physiotherapy. *Composites, Part A* **2022**, *152*, 106700.
(120) Hasan, M. M.; Hossain, M. M.; Chowdhury, H. K. Two-dimensional MXene-based flexible nanostructures for functional nanodevices: a review. *J. Mater. Chem. A* **2021**, *9* (6), 3231−3269.
(121) Sharifuzzaman, M.; Zahed, M. A.; Reza, M. S.; Asaduzzaman, M.; Jeong, S.; Song, H.; Kim, D. K.; Zhang, S.; Park, J. Y. MXene/Fluoropolymer-Derived Laser-Carbonaceous All-Fibrous Nanohybrid Patch for Soft Wearable Bioelectronics. *Adv. Funct. Mater.* **2023**, *33* (21), 2208894.
(122) Pei, Y.; Zhang, X.; Hui, Z.; Zhou, J.; Huang, X.; Sun, G.; Huang, W. Ti3C2TX MXene for sensing applications: recent progress, design principles, and future perspectives. *ACS Nano* **2021**, *15* (3), 3996−4017.
(123) Qin, R.; Nong, J.; Wang, K.; Liu, Y.; Zhou, S.; Hu, M.; Zhao, H.; Shan, G. Recent Advances in Flexible Pressure Sensors Based on MXene Materials. *Adv. Mater.* **2024**, *36* (24), 2312761.
(124) Wang, Y.; Wang, Y.; Jian, M.; Jiang, Q.; Li, X. MXene Key Composites: A New Arena for Gas Sensors. *Nano-Micro Lett.* **2024**, *16* (1), 209.
(125) Chen, R.; Pang, W.; Li, S.; Zhou, H.; Han, D.; Qin, K.; Ren, S.; Gao, Z. Recent advances and prospects in MOF/MXene sensors. *Sustainable Mater. Technol.* **2024**, *40*, No. e00935.
(126) Das, P.; Marvi, P. K.; Ganguly, S.; Tang, X.; Wang, B.; Srinivasan, S.; Rajabzadeh, A. R.; Rosenkranz, A. MXene-Based Elastomer Mimetic Stretchable Sensors: Design, Properties, and Applications. *Nano-Micro Lett.* **2024**, *16* (1), 135.
(127) Hamzehlouy, A.; Zarei, S.; Salah Othman, R.; Shahi, F.; Afshar, H.; Afshar Taromi, A.; Khonakdar, H. A. Recent Advances in Biomedical Applications of MXene-Integrated Electrospun Fibers: A Review. *Polym. Adv. Technol.* **2025**, *36* (2), No. e70112.
(128) Wang, T.; Zhu, L.; Yue, Y.; Mukai, Y.; Kanda, H.; Yamamoto, T. Fiber-optic sensor modified by electrospun Polymer/Ti3C2MXene−TiO2 for dimethyl sulfoxide sensing. *Talanta* **2025**, *287*, 127630.
(129) Fu, Y.; Liu, J.; Zou, J.; Xu, S.; Wei, Y.; Zhang, W.; Li, D. Electrospun PAN/BaTiO3/MXene nanofibrous membrane with significantly improved piezoelectric property for self-powered wearable sensor. *Chem. Eng. J.* **2024**, *489*, 151495.
(130) Ding, Y.; Huang, L.-Z.; Ji, X.-X.; Ma, M.-G. Utilizing electrospinning to fabricate porous polyvinylidene fluoride/cellulose nanocrystalline/MXene films for wearable pressure sensors. *Int. J. Biol. Macromol.* **2025**, *284*, 138106.
(131) Dinh Le, T.-S.; An, J.; Huang, Y.; Vo, Q.; Boonruangkan, J.; Tran, T.; Kim, S.-W.; Sun, G.; Kim, Y.-J. Ultrasensitive anti-interference voice recognition by bio-inspired skin-attachable self-cleaning acoustic sensors. *ACS Nano* **2019**, *13* (11), 13293−13303.
(132) Li, L.; Shi, P.; Hua, L.; An, J.; Gong, Y.; Chen, R.; Yu, C.; Hua, W.; Xiu, F.; Zhou, J.; et al. Design of a wearable and shape-memory fibriform sensor for the detection of multimodal deformation. *Nanoscale* **2018**, *10* (1), 118−123.
(133) Hui, Z.; Chen, R.; Chang, J.; Gong, Y.; Zhang, X.; Xu, H.; Sun, Y.; Zhao, Y.; Wang, L.; Zhou, R.; et al. Solution-processed sensing textiles with adjustable sensitivity and linear detection range enabled by twisting structure. *ACS Appl. Mater. Interfaces* **2020**, *12* (10), 12155−12164.
(134) Sivasankarapillai, V. S.; Sharma, T. S. K.; Hwa, K.-Y.; Wabaidur, S. M.; Angaiah, S.; Dhanusuraman, R. MXene based sensing materials: current status and future perspectives. *ES Energy Environ.* **2022**, *15*, 4−14.
(135) Guo, Z.; Li, Y.; Lu, Z.; Liu, W. Applications of MXene-based composite fibers in smart textiles. *J. Phys.: Conf. Ser.* **2021**, *1790*, 012066.
(136) Cantos-Prieto, F.; Falin, A.; Alliati, M.; Qian, D.; Zhang, R.; Tao, T.; Barnett, M. R.; Santos, E. J. G.; Li, L. H.; Navarro-Moratalla, E. Layer-Dependent Mechanical Properties and Enhanced Plasticity in the Van der Waals Chromium Trihalide Magnets. *Nano Lett.* **2021**, *21* (8), 3379−3385.
(137) Smriti, S. A.; Haque, A. N. M. A.; Khadem, A. H.; Siddiqa, F.; Rahman, A. N. M. M.; Himu, H. A.; Farzana, N.; Islam, M. A.; Naebe, M. Recent developments of the nanocellulose extraction from water hyacinth: a review. *Cellulose* **2023**, *30* (14), 8617−8641.
(138) Masudur Rahman, A. N. M.; Zhang, X.; Qin, X.; Smriti, S. A.; Khadem, A. H.; Ul Hasan, T.; Das, S. R.; Sharmin, F. A. Fabrication of novel cellulosic okra woven fabric and evaluation of its mechanical and coloration properties: an agricultural waste turning into valuable material. *Cellulose* **2023**, *30* (12), 8001−8022.
(139) Qin, L.; Yang, D.; Zhang, M.; Zhao, T.; Luo, Z.; Yu, Z.-Z. Superelastic and ultralight electrospun carbon nanofiber/MXene hybrid aerogels with anisotropic microchannels for pressure sensing and energy storage. *J. Colloid Interface Sci.* **2021**, *589*, 264−274.
(140) Bi, X.; Duan, Z.; Hou, X.; Qian, S.; Yuan, M.; Hu, J.; Zhang, J.; Lu, Y.; Liu, Y.; He, J.; Peng, Z.; Chou, X. Perpendicularly assembled oriented electrospinning nanofibers based piezoresistive pressure sensor with wide measurement range. *Nano Res.* **2024**, *17*, 6493−6501.
(141) Lee, E.; Kim, D.-J. Recent exploration of two-dimensional MXenes for gas sensing: From a theoretical to an experimental view. *J. Electrochem. Soc.* **2020**, *167* (3), 037515.
(142) Yu, X.-f.; Li, Y.-c.; Cheng, J.-b.; Liu, Z.-b.; Li, Q.-z.; Li, W.-z.; Yang, X.; Xiao, B. Monolayer Ti2CO2: a promising candidate for NH3 sensor or capturer with high sensitivity and selectivity. *ACS Appl. Mater. Interfaces* **2015**, *7* (24), 13707−13713.

(143) Abu-Lebdeh, Y. *Nanotechnology for Lithium-Ion Batteries*; Springer SBM, 2012.
(144) Yao, L.; Tian, X.; Cui, X.; Zhao, R.; Xiao, M.; Wang, B.; Xiao, X.; Wang, Y. Two-dimensional Ti3C2Tx MXene/SnO nanocomposites: Towards enhanced response and selective ammonia vapor sensor at room temperature. *Sens. Actuators, B* **2022**, *358*, 131501.
(145) Bhargava Reddy, M. S.; Kailasa, S.; Marupalli, B. C. G.; Sadasivuni, K. K.; Aich, S. A Family of 2D-MXenes: Synthesis, Properties, and Gas Sensing Applications. *ACS Sens.* **2022**, *7* (8), 2132−2163.
(146) Ali, I.; Faraz Ud Din, M.; Gu, Z.-G. MXenes thin films: from fabrication to their applications. *Molecules* **2022**, *27* (15), 4925.
(147) Sardana, S.; Mahajan, A. Highly Flexible, Selective and Sensitive Ammonia Sensor Based on MXene/Cellulose Nanofibers. *J. Electron. Mater.* **2024**, *53*, 4939−4946.
(148) Ma, S.; Guo, J.; Zhang, H.; Shao, X.; Zhang, D. A Room Temperature Trimethylamine Gas Sensor Based on Electrospinned Molybdenum Oxide Nanofibers/Ti3C2Tx MXene Heterojunction. *Nanomater* **2024**, *14*, 537.
(149) Xie, Q.; Ding, Y.; Wang, Q.; Song, P. Fabrication of 1D/2D In2O3 nanofibers/Ti3C2TX MXene composites for high performance detection of trimethylamine at low temperature. *Sens. Actuators, B* **2024**, *405*, 135338.
(150) Sun, B.; Ding, Y.; Wang, Q.; Song, P. Rational design of 1D/2D heterostructured ZnSnO3/ZnO/Ti3C2TX MXene nanocomposites for enhanced acetone gas sensing performance. *Sens. Actuators, B* **2024**, *409*, 135541.
(151) Sun, B.; Liu, M.; Liu, L.; Wang, Q.; Song, P. Synthesis of 1D LaFeO3 nanofibers/2D MXene heterostructures for formaldehyde detection at low temperature. *Sens. Actuators, B* **2024**, *415*, 136011.
(152) Gasso, S.; Mahajan, A. Self-Powered Wearable Gas Sensors Based on l-Ascorbate-Treated MXene Nanosheets and SnO2 Nanofibers. *ACS Appl. Nano Mater.* **2023**, *6* (8), 6678−6692.
(153) Mirzaei, A.; Kim, J.-Y.; Kim, H. W.; Kim, S. S. Resistive Gas Sensors Based on 2D TMDs and MXenes. *Acc. Chem. Res.* **2024**, *57* (16), 2395−2413.
(154) Bhardwaj, R.; Hazra, A. SrTiO3 passivated MXene (Ti3C2Tx) for efficient VOC detection in hazardous humid ambient. *Sens. Actuators, B* **2024**, *401*, 134967.
(155) Siraj, S.; Bansal, G.; Hasita, B.; SrungaramRybicki, S. F. J.; Sonkusale, S.; Sahatiya, P.; Sahatiya, P. MXene/MoS2 Piezotronic Acetone Gas Sensor for Management of Diabetes. *ACS Appl. Nano Mater.* **2024**, *7* (10), 11350−11361.
(156) Shi, S.; Si, Y.; Li, Z.; Meng, S.; Zhang, S.; Wu, H.; Zhi, C.; Io, W.-F.; Ming, Y.; Wang, D.; et al. An intelligent wearable filtration system for health management. *ACS Nano* **2023**, *17* (7), 7035−7046.
(157) Zhu, M.; Yu, J.; Li, Z.; Ding, B. Self-healing fibrous membranes. *Angew. Chem., Int. Ed.* **2022**, *61* (41), No. e202208949.
(158) Zhi, C.; Shi, S.; Meng, S.; Wu, H.; Si, Y.; Zhang, K.; Zhang, S.; Hu, J. A biocompatible and antibacterial all-textile structured triboelectric nanogenerator for self-powered tactile sensing. *Nano Energy* **2023**, *115*, 108734.
(159) Zhang, J.; Yang, T.; Tian, G.; Lan, B.; Deng, W.; Tang, L.; Ao, Y.; Sun, Y.; Zeng, W.; Ren, X.; Li, Z.; Jin, L.; Yang, W. Spatially Confined MXene/PVDF Nanofiber Piezoelectric Electronics. *Adv. Fiber Mater.* **2024**, *6* (1), 133−144.
(160) Yin, J.; Wang, J.; Ramakrishna, S.; Xu, L. All-Electrospun Triboelectric Nanogenerator Incorporating Carbon-Black-Loaded Nanofiber Membranes for Self-Powered Wearable Sensors. *ACS Appl. Nano Mater.* **2023**, *6* (17), 15416−15425.
(161) Pan, C.-T.; Dutt, K.; Kumar, A.; Kumar, R.; Chuang, C.-H.; Lo, Y.-T.; Wen, Z.-H.; Wang, C.-S.; Kuo, S.-W. PVDF/AgNP/MXene composites-based near-field electrospun fiber with enhanced piezoelectric performance for self-powered wearable sensors. *Int. J. Bioprint.* **2022**, *9* (1), 647.
(162) Rana, S. M.; Toyabur Rahman, M.; Salauddin, M.; Cho, H.; Park, J. Y. An Electrospun PVDF-TRFE/Mxene Nanofibours Mat-Based Self-Powered Motion Sensor. In *IEEE 34th International Conference on Micro Electro Mechanical Systems (MEMS)*, 2021, pp 30−33..
(163) Wang, W.; Xu, L.; Zhang, L.; Zhang, A.; Zhang, J. Self-Powered Integrated Sensing System with In-Plane Micro-Supercapacitors for Wearable Electronics. *Small* **2023**, *19* (29), 2207723.
(164) Scheibe, B. e.; Wychowaniec, J. K.; Scheibe, M.; Peplinska, B.; Jarek, M.; Nowaczyk, G.; Przysiecka, Ł. Cytotoxicity assessment of Ti−Al−C based MAX phases and Ti3C2T x MXenes on human fibroblasts and cervical cancer cells. *ACS Biomater. Sci. Eng.* **2019**, *5* (12), 6557−6569.
(165) Li, D.-D.; Yuan, Q.; Huang, L.-Z.; Zhang, W.; Guo, W.-Y.; Ma, M.-G. Preparation of flexible N-doped carbon nanotube/MXene/PAN nanocomposite films with improved electrochemical properties. *Ind. Eng. Chem. Res.* **2021**, *60* (42), 15352−15363.
(166) Ranjith, K. S.; Vilian, A. T. E.; Ghoreishian, S. M.; Umapathi, R.; Huh, Y. S.; Han, Y.-K. An ultrasensitive electrochemical sensing platform for rapid detection of rutin with a hybridized 2D-1D MXene-FeWO4 nanocomposite. *Sens. Actuators, B* **2021**, *344*, 130202.
(167) Ranjith, K. S.; Vilian, A. T. E.; Ghoreishian, S. M.; Umapathi, R.; Hwang, S.-K.; Oh, C. W.; Huh, Y. S.; Han, Y.-K. Hybridized 1D−2D MnMoO4−MXene nanocomposites as high-performing electrochemical sensing platform for the sensitive detection of dihydroxybenzene isomers in wastewater samples. *J. Hazard. Mater.* **2022**, *421*, 126775.
(168) Mohseni Taromsari, S.; Shi, H. H.; Habibpour, S.; Kiddell, S.; Yu, A.; Park, C. B.; Naguib, H. E. An ultra-sensitive and stable electrochemical sensor with an expanded working range via in situ assembly of 3-D structures based on MXene/GnR nanohybrids. *J. Mater. Chem. A* **2023**, *11* (20), 10748−10765.
(169) Zong, C.-M.; Zhang, B.; Li, S.-Y.; Jin, J.; Lu, Z.-Z.; Yao, X.-H.; Zhao, W.-G.; Chen, T.; Zhang, D.-Y. A flexible multifunctional sensor with a conductive network based on silk nanofibers and MXene for monitoring physiological activity, capacitive pens, photothermal conversion and antibacterial. *Int. J. Biol. Macromol.* **2025**, *305*, 141148.
(170) Tang, Y.; Yan, J.; Wang, J.; Liu, Y.; Zhang, G.; Huang, X.; Xue, H.; Gao, J. Mechanically durable MXene based nanofiber composite membranes with asymmetric superhydrophilicity/hydrophobicity for unidirectional water transport and temperature sensing. *Chem. Eng. J.* **2024**, *480*, 148034.
(171) Hu, J.; Wang, X.; Lei, H.; Luo, M.; Zhang, Y. Plasmonic photothermal driven MXene-based gas sensor for highly sensitive NO2 detection at room temperature. *Sens. Actuators, B* **2024**, *407*, 135422.
(172) Mao, M.; Kong, J.; Ge, X.; Sun, Y.; Yu, H.; Liu, J.; Huang, W.; Wang, D. Y.; Wang, Y. Mxene-based wearable self-powered and photothermal triboelectric nanogenerator patches for wound healing acceleration and tactile sensing. *Chem. Eng. J.* **2024**, *482*, 148949.
(173) Chao, M.; Di, P.; Yuan, Y.; Xu, Y.; Zhang, L.; Wan, P. Flexible breathable photothermal-therapy epidermic sensor with MXene for ultrasensitive wearable human-machine interaction. *Nano Energy* **2023**, *108*, 108201.
(174) Siwal, S. S.; Kaur, H.; Chauhan, G.; Thakur, V. K. MXene-Based Nanomaterials for Biomedical Applications: Healthier Substitute Materials for the Future. *Adv. Nanobiomed Res.* **2023**, *3* (1), 2200123.
(175) Li, H.; Fan, R.; Zou, B.; Yan, J.; Shi, Q.; Guo, G. Roles of MXenes in biomedical applications: recent developments and prospects. *J. Nanobiotechnol.* **2023**, *21* (1), 73.
(176) Dmytriv, T. R.; Lushchak, V. I. Potential Biosafety of Mxenes: Stability, Biodegradability, Toxicity and Biocompatibility. *Chem. Rec.* **2024**, *24* (4), No. e202300338.
(177) Rakhi, R. B.; Nayak, P.; Xia, C.; Alshareef, H. N. Novel amperometric glucose biosensor based on MXene nanocomposite. *Sci. Rep.* **2016**, *6* (1), 36422.
(178) Gu, H.; Xing, Y.; Xiong, P.; Tang, H.; Li, C.; Chen, S.; Zeng, R.; Han, K.; Shi, G. Three-Dimensional Porous Ti3C2Tx MXene−Graphene Hybrid Films for Glucose Biosensing. *ACS Appl. Nano Mater.* **2019**, *2* (10), 6537−6545.
(179) Huang, K.; Li, Z.; Lin, J.; Han, G.; Huang, P. Two-dimensional transition metal carbides and nitrides (MXenes) for biomedical applications. *Chem. Soc. Rev.* **2018**, *47* (14), 5109−5124.

https://doi.org/10.1021/acsanm.5c02646
ACS Appl. Nano Mater. 2025, 8, 16231−16259

(180) Chen, K.; Qiu, N.; Deng, Q.; Kang, M.-H.; Yang, H.; Baek, J.-U.; Koh, Y.-H.; Du, S.; Huang, Q.; Kim, H.-E. Cytocompatibility of Ti3AlC2, Ti3SiC2, and Ti2AlN: in vitro tests and first-principles calculations. *ACS Appl. Bio Mater.* **2017**, *3* (10), 2293−2301.
(181) Shen, Y.; Chai, S.; Zhang, Q.; Zhang, M.; Mao, X.; Wei, L.; Zhou, F.; Sun, R.; Liu, C. PVF composite conductive nanofibers-based organic electrochemical transistors for lactate detection in human sweat. *Chem. Eng. J.* **2023**, *475*, 146008.
(182) Zizhou, R.; Baratchi, S.; Khoshmanesh, K.; Wang, X.; Houshyar, S. PMMA/PDMS/MXene Nanofibers for Postsurgery Monitoring of Vascular Implants. *ACS Appl. Nano Mater.* **2024**, *7* (8), 9757−9767.
(183) Huang, J.; Xie, G.; Wei, Q.; Su, Y.; Xu, X.; Jiang, Y. Degradable MXene-Doped Polylactic Acid Textiles for Wearable Biomonitoring. *ACS Appl. Mater. Interfaces* **2023**, *15* (4), 5600−5607.
(184) Quan, W.; Shi, J.; Luo, H.; Fan, C.; Lv, W.; Chen, X.; Zeng, M.; Yang, J.; Hu, N.; Su, Y.; Wei, H.; Yang, Z. Fully Flexible MXene-based Gas Sensor on Paper for Highly Sensitive Room-Temperature Nitrogen Dioxide Detection. *ACS Sens.* **2023**, *8* (1), 103−113.
(185) Majhi, S. M.; Ali, A.; Greish, Y. E.; El-Maghraby, H. F.; Qamhieh, N. N.; Hajamohideen, A. R.; Mahmoud, S. T. Accordion-like-Ti3C2MXene-Based Gas Sensors with Sub-ppm Level Detection of Acetone at Room Temperature. *ACS Appl. Electron. Mater.* **2022**, *4* (8), 4094−4103.
(186) Yi, Q.; Pei, X.; Das, P.; Qin, H.; Lee, S. W.; Esfandyarpour, R. A self-powered triboelectric MXene-based 3D-printed wearable physiological biosignal sensing system for on-demand, wireless, and real-time health monitoring. *Nano Energy* **2022**, *101*, 107511.
(187) Wang, D.; Zhang, D.; Tang, M.; Zhang, H.; Chen, F.; Wang, T.; Li, Z.; Zhao, P. Rotating triboelectric-electromagnetic nanogenerator driven by tires for self-powered MXene-based flexible wearable electronics. *Chem. Eng. J.* **2022**, *446*, 136914.
(188) Salauddin, M.; Rana, S. M. S.; Rahman, M. T.; Sharifuzzaman, M.; Maharjan, P.; Bhatta, T.; Cho, H.; Lee, S. H.; Park, C.; Shrestha, K.; Sharma, S.; Park, J. Y. Fabric-Assisted MXene/Silicone Nanocomposite-Based Triboelectric Nanogenerators for Self-Powered Sensors and Wearable Electronics. *Adv. Funct. Mater.* **2022**, *32* (5), 2107143.
(189) Zhang, Y.; Wang, L.; Zhao, L.; Wang, K.; Zheng, Y.; Yuan, Z.; Wang, D.; Fu, X.; Shen, G.; Han, W. Flexible Self-Powered Integrated Sensing System with 3D Periodic Ordered Black Phosphorus@MXene Thin-Films. *Adv. Mater.* **2021**, *33* (22), 2007890.
(190) Xiao, P.; Zhu, G.; Shang, X.; Hu, B.; Zhang, B.; Tang, Z.; Yang, J.; Liu, J. An Fe-MOF/MXene-based ultra-sensitive electrochemical sensor for arsenic(III) measurement. *J. Electroanal. Chem.* **2022**, *916*, 116382.
(191) Gopal, T. S.; Jeong, S. K.; Alrebdi, T. A.; Pandiaraj, S.; Alodhayb, A.; Muthuramamoorthy, M.; Andrews Nirmala, G. MXene-based composite electrodes for efficient electrochemical sensing of glucose by non-enzymatic method. *Mater. Today Chem.* **2022**, *24*, 100891.
(192) Bhat, K. S.; Byun, S.; Alam, A.; Ko, M.; An, J.; Lim, S. A fast and label-free detection of hydroxymethylated DNA using a nozzle-jet printed AuNPs@Ti3C2MXene-based electrochemical sensor. *Talanta* **2022**, *244*, 123421.
(193) Rizwan, K.; Rahdar, A.; Bilal, M.; Iqbal, H. M. N. MXene-based electrochemical and biosensing platforms to detect toxic elements and pesticides pollutants from environmental matrices. *Chemosphere* **2022**, *291*, 132820.
(194) Momeni, F.; Khoshfetrat, S. M.; Bagheri, H.; Zarei, K. Ti3C2MXene-based nanozyme as coreaction accelerator for enhancing electrochemiluminescence of glucose biosensing. *Biosens. Bioelectron.* **2024**, *250*, 116078.
(195) Mathew, M.; Rout, C. S. Electrochemical biosensors based on Ti3C2Tx MXene: future perspectives for on-site analysis. *Curr. Opin. Electrochem.* **2021**, *30*, 100782.
(196) Chaudhary, V.; Khanna, V.; Ahmed Awan, H. T.; Singh, K.; Khalid, M.; Mishra, Y. K.; Bhansali, S.; Li, C.-Z.; Kaushik, A. Towards hospital-on-chip supported by 2D MXenes-based 5th generation intelligent biosensors. *Biosens. Bioelectron.* **2023**, *220*, 114847.
(197) Sarmah, H. S.; Ghosh, S. Surface Passivation and Tunable Magnetic Properties of Cr-Based MXenes. *J. Phys. Chem. C* **2024**, *128* (38), 16133−16142.
(198) Kumar, S. S.; H, R.; Hattrup, N.; Wang, G. J.; Presto, A. A.; Reeja-Jayan, B. Polymer encapsulation via initiated chemical vapor deposition (iCVD) to enhance stability of $Ti_3C_2T_x$ MXene-based formaldehyde sensors. *Sci. Adv.* **2025**, *11* (28), No. eadu6682.
(199) Kumar, S.; Kumari, N.; Singh, T.; Seo, Y. Shielding 2D MXenes against oxidative degradation: recent advances, factors and preventive measures. *J. Mater. Chem. C* **2024**, *12* (23), 8243−8281.
(200) Tian, Y.; Hou, P.; Zhang, H.; Xie, Y.; Chen, G.; Li, Q.; Du, F.; Vojvodic, A.; Wu, J.; Meng, X. Theoretical insights on potential-dependent oxidation behaviors and antioxidant strategies of MXenes. *Nat. Commun.* **2024**, *15* (1), 10099.
(201) Eghbali, P.; Hassani, A.; Wacławek, S.; Andrew Lin, K.-Y.; Sayyar, Z.; Ghanbari, F. Recent advances in design and engineering of MXene-based catalysts for photocatalysis and persulfate-based advanced oxidation processes: A state-of-the-art review. *Chem. Eng. J.* **2024**, *480*, 147920.
(202) Yang, Y.; Yang, S.; Xia, X.; Hui, S.; Wang, B.; Zou, B.; Zhang, Y.; Sun, J.; Xin, J. H. MXenes for Wearable Physical Sensors toward Smart Healthcare. *ACS Nano* **2024**, *18* (36), 24705−24740.
(203) Chen, R.; Jia, X.; Zhou, H.; Ren, S.; Han, D.; Li, S.; Gao, Z. Applications of MXenes in wearable sensing: Advances, challenges, and prospects. *Mater. Today* **2024**, *75*, 359−385.
(204) Wang, Y.; Wang, Y.; Kuai, Y.; Jian, M. "Visualization" Gas—Gas Sensors Based on High Performance Novel MXenes Materials. *Small* **2024**, *20* (2), 2305250.
(205) Shahzad, F.; Zaidi, S. A.; Naqvi, R. A. 2D transition metal carbides (MXene) for electrochemical sensing: A review. *Crit. Rev. Anal. Chem.* **2022**, *52* (4), 848−864.
(206) Zhang, S.; Meng, L.; Hu, Y.; Yuan, Z.; Li, J.; Liu, H. Green synthesis and biosafety assessment of MXene. *Small* **2024**, *20* (14), 2308600.